Chapter 2

GROWTH AND FORM

The raw materials of paleontology are individual specimens that we collect and prepare for study. Virtually all questions addressed with fossil data, whether geological, ecological, or evolutionary, rest ultimately upon detailed observation of individual specimens. To cite just a few examples:

1. We may wish to test the hypothesis that body size tends to increase over evolutionary time [SEE SECTION 7.4]. If so, we need to know what we mean by size and how to measure it.
2. Studies in systematics [SEE SECTIONS 3.3 AND 4.1], biostratigraphy [SEE SECTION 6.1], and biodiversity [SEE SECTION 8.1] require that paleontologists be able to assign specimens correctly to species, to know whether two specimens belong to the same or to different species, and to determine how many species are represented in a collection of specimens. Such studies depend on detailed description and measurement of these specimens.
3. If we want to interpret the mechanics, physiology, and ecology of extinct organisms [SEE SECTIONS 5.2 AND 9.4], we must understand the principles by which function depends on size and shape change through growth.

Although chemical, mineralogical, and other kinds of data are often collected from fossil specimens, the principal information typically concerns their form. We therefore begin this chapter with an elementary treatment of **morphology,** the study of biological form and structure.

2.1 ASPECTS OF FORM

Whether we are studying a whole organism or just one of its parts, there are three components of form to consider: size, shape, and the relationship between size and shape. **Size** is perhaps the most obvious biological trait. Not only is size obvious, but it is also of fundamental importance to the organism. Many aspects of function—such as metabolism, reproduction, and locomotion—vary regularly with size. Biologists can therefore predict much about an organism just by knowing how big it is. Given that an elephant is a mobile terrestrial animal with a large body mass, a biologist need never have seen one to be able to state with some confidence that it must have stout limbs vertically oriented below its body.

The second major component of organic form is **shape.** Intuitively, shape reflects the relative proportions of different parts of an organism. The length and breadth of a bone are measures of its size. By contrast, the ratio of the length to breadth—relatively slender versus relatively stout—is a measure of shape. Strictly speaking, a shape measure is derived as a ratio among other measures that have specific dimensions—usually mass (M), length (L), area (L^2), and volume (L^3)—in such a way that the dimensions cancel out to yield a dimensionless number. (The dimensions are distinct from the specific units, such as grams for mass and centimeters for length.) Both bone length and breadth have dimensions of length, L. Therefore, the ratio between them has dimensions $L \div L$, which equals L^0 and so is dimensionless. Not all ratios among size measures yield measures of shape. For example, the ratio between mass and volume

has the dimensions of density, namely $M \div L^3$ or ML^{-3}. Likewise, the ratio of bone cross-sectional area to bone length has dimensions $L^2 \div L$, which is equal to L.

An obvious aspect of shape is symmetry. Many familiar animals are bilaterally symmetrical (essentially identical from left to right) or radially symmetrical (similar in form in any direction perpendicular to the anterior–posterior axis). Other forms of symmetry exist, such as the fivefold symmetry of echinoderms. Basic symmetry is generally invariant within species, genera, and even higher taxa.

Shape typically changes as an organism grows, which brings us to the third component of form: the relationship between size and shape. The ways in which shape changes with size often reflect how organisms function, as we will see when we discuss the nature of growth and development.

2.2 DESCRIBING AND MEASURING SPECIMENS

What we measure and with what precision depend ultimately on the question being addressed. Prior experience studying a particular group of organisms is often essential in guiding the choice of measurements. It is therefore difficult to provide a single formula that will serve well for describing and measuring any specimen or species. Sometimes a simple measure of body size can discriminate two closely related species, but in other cases the species may be nearly identical in size, so that more detailed measurements will be necessary to distinguish them.

Which measures work best for which purposes will be developed by example during the course of this book and through the reading of case studies and examination of material in the laboratory. Two guidelines usually apply: (1) Within-species studies require higher precision than comparisons between different species, because the morphological differences are more subtle, and (2) the greater the level of detail in a system of description or measurement, the smaller the range of species to which that system can be applied. The simple height:width ratio can be compared among all shelled gastropods, for example, but measurements of particular aspects of ornamentation would apply only to those species that possess the ornament in question. Here we emphasize description and measurement of specimens that have already been collected and prepared for study. References at the end of the chapter and in the bibliography should be consulted for techniques of paleontological collection and preparation.

Pictorial Description

Except for the smallest of fossilized microorganisms, nearly all initial observations on specimens are made with the naked eye. Rich detail can often be documented with nothing more sophisticated than paper, pencil, and patience. Nonetheless, the structures we wish to study may be so small that they require a magnifying lens, optical microscope, or electron microscope. Or they may not be visible on the exterior of the specimen. Sectioning allows observations on interior structures, but this is destructive. Radiography, computerized axial tomography (CAT) scanning, and related methods allow one to gain a visual image of the interior of a specimen without damaging it. Such methods typically detect contrasts in density or composition, such as that between actual skeletal material and the sedimentary matrix. Figures 1.11 and 2.1 show examples of nondestructive imaging of fossils.

Once we can see a specimen, there are many tools that help us keep a permanent record of that specimen for future study or to aid measurement. In addition to the photograph, one of the most useful tools is the **camera lucida.** This is an optical device, sometimes attached to a microscope, that facilitates drawing by allowing one to see the image of the specimen superimposed on the image of one's hand. The sketch or line drawing is still an extremely important tool in the description of specimens. In cases in which material has suffered substantial post-mortem disarticulation and distortion, for example, it is absolutely essential to draw the specimen in such a way that the relevant biological detail is emphasized to the exclusion of taphonomic features.

The importance of the line drawing is illustrated in Figure 2.2. Figure 2.2a shows a specimen of the arthropod *Marrella splendens*, the most abundant species known from the Middle Cambrian Burgess Shale of British Columbia [SEE SECTION 10.2]. The specimen is distorted and partially obscured by sediment. Moreover, the color contrast between the specimen and the sedimentary matrix is somewhat limited, making it hard to distinguish the specimen from the sediment. Figure 2.2b is a line drawing of the specimen, made with the aid of a microscope and camera lucida. This drawing has elements of both faithful representation

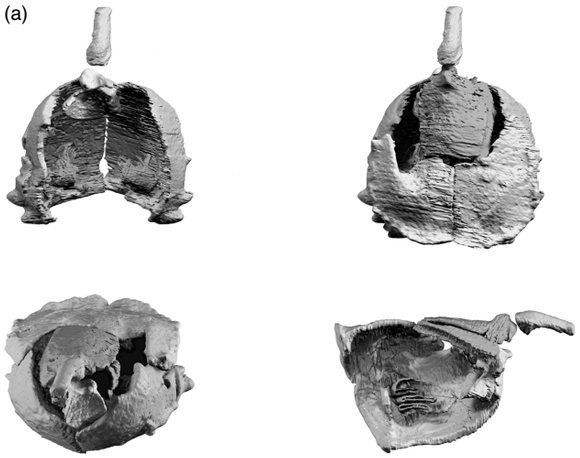

FIGURE 2.1 Nondestructive imaging of fossils. (a) A mitrate echinoderm from the Upper Carboniferous of Oklahoma, shown in four different orientations. Numerous, fine-scale X-ray images were taken to simulate serial sectioning without damaging the specimen. These serial images were then reconstructed in three dimensions via computer. (b) Magnetic resonance image (MRI) of the complex, three-dimensional trace fossil *Macaronichnus* from the Cretaceous of Alberta. *(a: From Dominguez et al., 2002; b: From Gingras et al., 2002, Permission by Society for Sedimentary Geology)*

and interpretation. The artist has tried to portray only the anatomical details that are actually evident. At the same time, given such problems as specimen distortion and obstruction by matrix, a certain degree of interpretation is inevitable. By studying many specimens preserved in different orientations, and making a line drawing of each, the reconstruction of Figure 2.2c was possible. Such a reconstruction is far more interpretative than any single line drawing; it portrays an idealized individual that is far more complete and symmetrical than any single specimen.

There are numerous systems that allow one to **digitize** specimens, that is, to store electronic images of

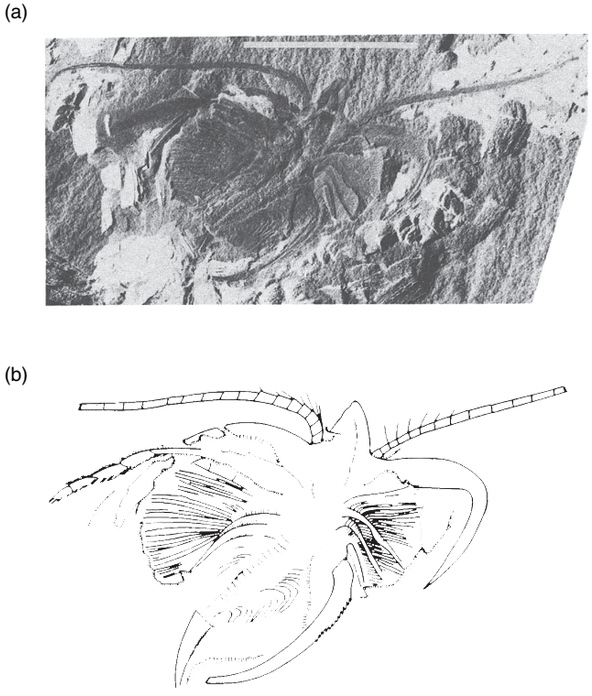

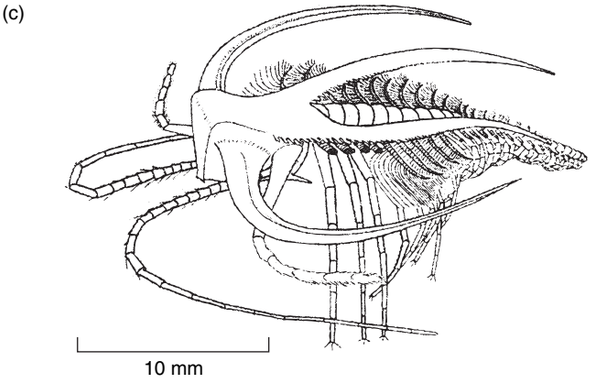

FIGURE 2.2 Images of the arthropod *Marrella splendens* from the Middle Cambrian of British Columbia. (a) Photograph of a specimen. (b) Line drawing of this same specimen, made with the aid of a camera lucida. (c) Reconstruction based on camera-lucida drawings of several specimens. *(From Whittington, 1971)*

(a)

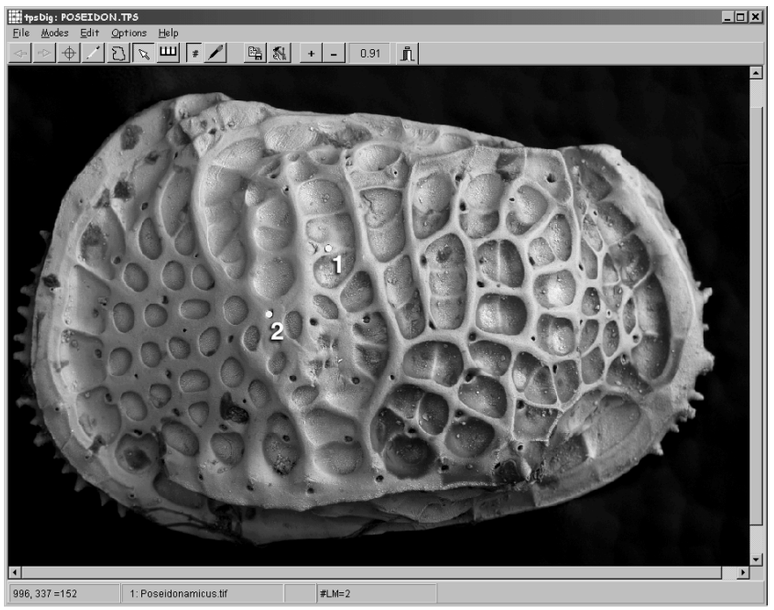

(b)

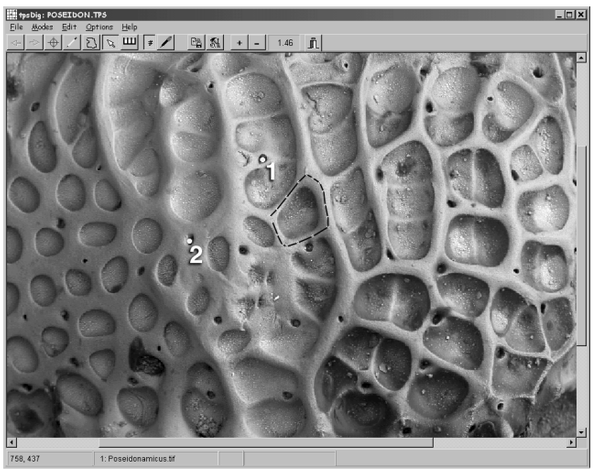

FIGURE 2.3 Digitized image of the left valve of the OSTRACODE *Poseidonamicus*, displayed with the computer software tpsDig. This image was produced with a scanning electron microscope. (a) Overview of a specimen showing two points, marked 1 and 2, that have been selected to have their *x*- and *y*-coordinates automatically recorded. Note the relative magnification of 0.91 indicated near the top of the computer screen. (b) Part of this same specimen at a relative magnification of 1.46. In addition to the points 1 and 2, a polygon has been traced around one of the fossae (the shallow depressions) on the valve. The area and geometric centroid of this polygon can be computed by the software. *(Courtesy of Gene Hunt)*

them. Digitization can be manual, in which case a specimen is drawn with a special stylus whose motion is mechanically or electronically recorded in two or three dimensions. More commonly, an entire photographic image is stored electronically. Automated storage of three-dimensional images can be accomplished by digitizing many closely spaced, thin sections, as in Figure 2.1a. It is also possible to digitize pairs of photographs taken at slightly different angles—which simulates binocular vision—and to use computer algorithms to reconstruct the form trigonometrically. Manual digitization is often more laborious than automated methods, but, like the line drawing relative to the photograph, it has the advantage that only the desired detail is recorded.

Modern digitizing equipment has high optical resolution and can reduce the distortion that inevitably results from projecting a three-dimensional specimen into two dimensions. Moreover, there are many sophisticated and versatile computer programs to work with digitized images. Photographic images can be processed to remove unwanted detail and therefore to make measurement easier. For example, the contrast between a light-colored specimen and a dark background can be exploited to approximate the outline of the specimen so that this need not be traced by hand. Many standard measurements can be recorded with little effort using computer programs. In an important sense, therefore, having a properly digitized image is like having the actual specimen at hand (see Figure 2.3).

Digitization and computer software facilitate specimen description and measurement. They do not, however, solve the important problem of deciding *what* to describe and measure. We now turn to this question.

Descriptive Terminology

By far the most common medium for describing a structure is the word. Well-designed terminology can powerfully and economically describe form, reducing a great deal of information to a single word or relatively few words. If carefully chosen, the words are self-explanatory and relatively easy to learn.

FIGURE 2.4 Cretaceous gastropod *Calliomphalus conanti*. See text for the formal description of this species. *(From Sohl, 1960)*

As an example of the effective use of descriptive terminology, the formal description of a gastropod species follows (from Sohl, 1960). Photographs of a specimen of the species are shown in Figure 2.4.

> Shell small, trochiform, phaneromphalous with nacreous inner shell layer; holotype with about $7\frac{1}{4}$ rapidly expanding whorls. Protoconch smooth on early whorl with coarse axial costae appearing at slightly more than one whorl, followed almost immediately by fine spiral lirae; suture impressed. Whorl sides slope less steeply than general slope of spire, giving an outline interrupted by overhang of periphery of preceding whorls; periphery subround to subangular; whorl side slopes steeply below periphery to broadly rounded base. Sculpture of axial and spiral elements same size; 8 spiral lirae on upper slope possess subdued tubercles where overridden by somewhat coarser and closer spaced axial cords; base covered by about 10 unequally spaced spirals with poorly defined tubercles and numerous axial lirae. Umbilicus narrow, bordered by a margin bearing low nodes. Aperture incompletely known, subcircular, slightly wider than high and reflexed slightly at junction of inner lip and umbilical margin.

To a person unfamiliar with gastropod morphology and its descriptive terminology, this description may be nearly unintelligible. For the person acquainted with the subject, however, the description should provide a convincing sketch of a group of specimens.

Any system of descriptive terminology can lead to difficulty. For example, note the word *small* in the first line of the description. This implies a size comparison with other organisms—but what other organisms? By convention, terms such as *small*, *large*, *wide*, and *narrow* imply comparison only with closely related organisms.

Descriptive terminology often includes a number of categories to which the principal forms in a biologic group can be assigned. Figure 2.5 shows some examples for gastropod shells. A common problem is deciding

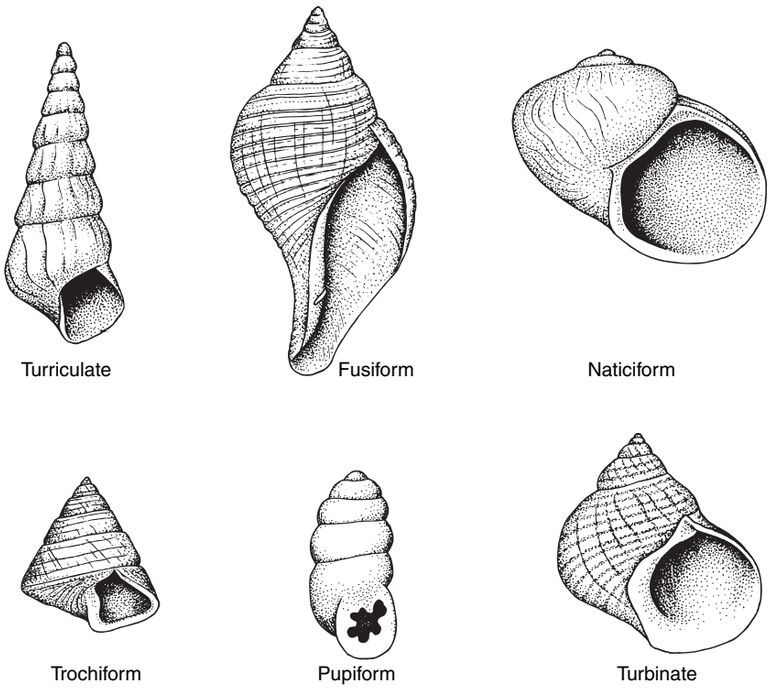

FIGURE 2.5 Some of the terms for shape used in morphologic descriptions of gastropods. The origin of such terms, some of which are several centuries old, is quite varied. Some terms are derived from descriptive words: "Turbinate" comes from the Latin *turbinatus*, meaning "top-shaped." Others not shown here are from geometry: conical, biconical, obconical, and so on. Still others are derived from the names of particular taxa—"naticiform" from the genus *Natica*, for example.

where one category leaves off and another begins. What do we do, for example, if we are faced with a shell that is somewhere between naticiform and turbinate? One reason that intermediate forms do not present even more problems than they do is that biologic form is not randomly distributed [SEE SECTION 5.3]. Certain shapes are much more common than others. If a system of descriptive terminology accurately reflects the natural clusters of predominant forms, then relatively few specimens will be found that are between two categories. Thus, the establishment of a system of descriptive terminology may be an important scientific contribution in itself, representing a fundamental interpretation of the natural world.

Description by Measurement

The counting of **meristic characters** is a simple form of quantitative description. Examples include the number of ribs in a fish, the number of petals in a flower, and the number of segments in an arthropod. Such a tabulation may seem crude, but it can be quite informative. For example, it is possible to distinguish among many groups of trilobites based on the number of segments, and species within certain groups of trilobites are characterized by a specific number of pits on the fringe of the head.

Most quantitative description of fossils involves measurement in the strict sense rather than counting. As a simple example, consider the leaves portrayed in Figure 2.6, along with one shape measure, the length:width ratio. The leaves are nearly identical in this measure but obviously differ substantially in other aspects of shape. To describe form with nothing more than the length:width ratio implicitly assumes that a rectangle is a good approximation to the form—in other words, that it is reasonable to use the rectangle as an idealized model of form. In fact, any system of measurement assumes a model of some sort.

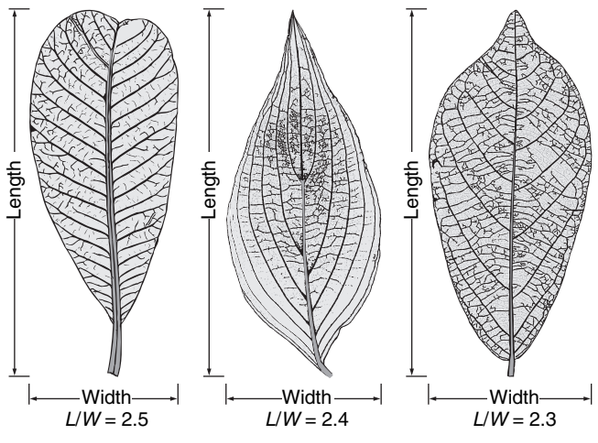

FIGURE 2.6 Leaves of three different tree species, with length and width indicated. These leaves have approximately the same length:width ratio, but they differ in other aspects of shape. *(From Leaf Architecture Working Group, 1999)*

Four hypothetical coiled **CEPHALOPODS** are shown in Figure 2.7. For each, the largest diameter, *d*, is indicated, which distinguishes the large forms from the small. The diameter, however, tells us little about shape. The model tacitly assumed is a circle. Any number of quite different spiral cephalopods can be inscribed in the same circle, and thus the diameter gives us little indication of anything except size. For each of the shapes in Figure 2.7, a pair of unequal radii (r_1 and r_2), each originating in the morphologic center of the spiral, gives us more information. For these hypothetical forms, the ratio of any two radii measured at equal angular intervals, in this case 180 degrees, is a constant value. This means that, with respect to these radii, the shape of the shell is not changing with growth. Many real shells conform approximately to an ideal model with constant ratios of radii. Based on the ratio of radii, we can distinguish three cephalopod forms. The ratio of the two radii in Figure 2.7a is larger than their ratio in Figure 2.7d, and this reflects some of the differences between the two shapes. The differences between Figures 2.7b and 2.7c are evident in the drawings, but these two forms are indistinguishable from each other by the ratios of radii.

The foregoing examples illustrate the simplest and still most commonly used approach to quantitative description: the measurement of a series of linear size dimensions, and the definition of shape variables based on ratios among these. This approach has a number of advantages. It yields measures that are intuitively satisfying and correspond to the aspects of form that commonly strike the eye of both the expert and the beginner. It can be carried out quickly and easily with only minimal equipment, such as a ruler or calipers. And it allows a wide range of forms to be compared, provided that the measures are carefully chosen. Perhaps the main shortcoming of this approach is that complex analyses, some of which we discuss in the next chapter, may be required to interpret the data if one has taken many measurements on each specimen in an effort to describe the form in great detail. Biologically realistic models, such as that for the coiled shell, can therefore be of great value in allowing an economical set of measurements [SEE SECTION 5.3].

Related to the measurement of linear dimensions is the recording of *x*-, *y*-, and *z*-coordinates of reference

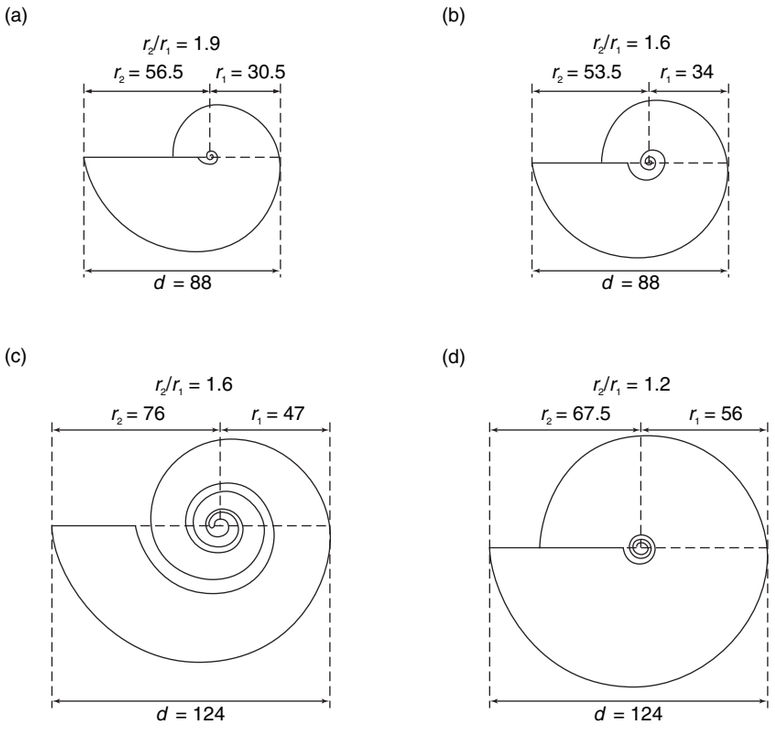

FIGURE 2.7 Four generalized shell forms common in coiled cephalopods. Parts (a) and (b) have the same diameter (d), as do parts (c) and (d). These diameters depict size but not shape. The ratio of radii, r_1/r_2, conveys considerable shape information. Parts (b) and (c) have the same ratio, however, even though they differ in other respects.

points or **landmarks** on the specimen. These landmarks may be, for example, the triple-point junctions of echinoderm plates or arthropod sclerites, the points of articulation of skeletal elements, or extreme points such as the tip of a limb. Figure 2.8 shows some examples of landmarks. In the case of the **OSTEICHTHYAN** fish (Figure 2.8a), the form is approximated by a two-dimensional projection. For the **BLASTOID** echinoderm (Figure 2.8b), a special microscope was used to record the coordinates of landmarks in three dimensions.

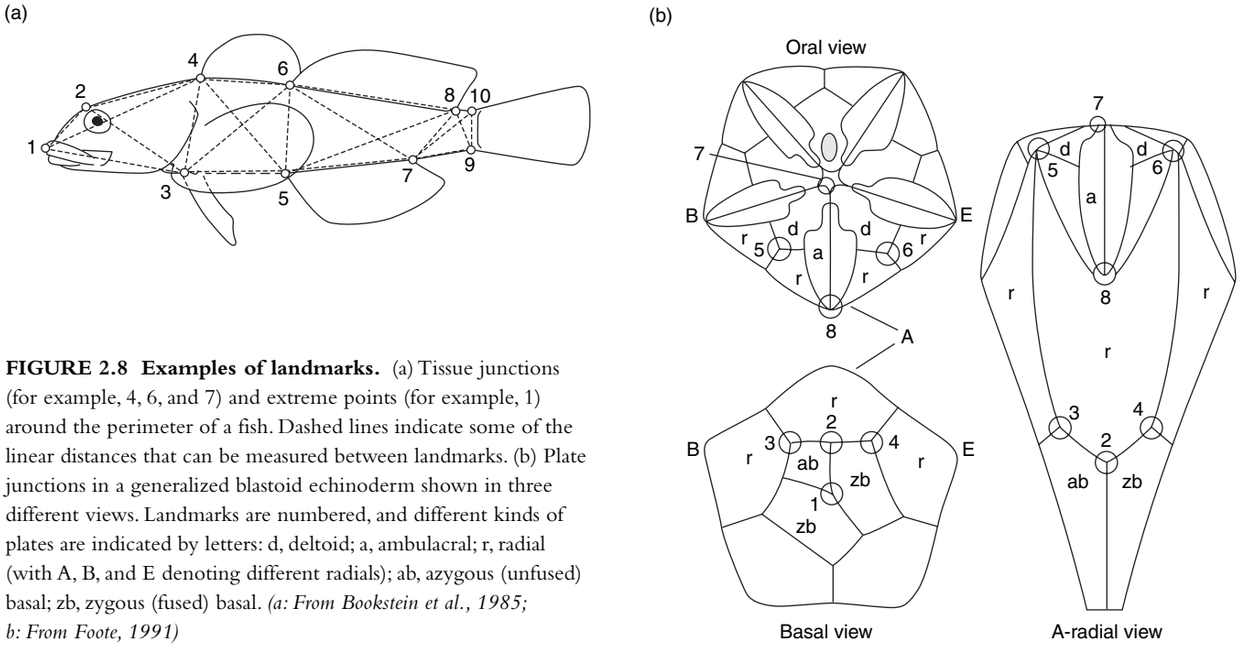

FIGURE 2.8 Examples of landmarks. (a) Tissue junctions (for example, 4, 6, and 7) and extreme points (for example, 1) around the perimeter of a fish. Dashed lines indicate some of the linear distances that can be measured between landmarks. (b) Plate junctions in a generalized blastoid echinoderm shown in three different views. Landmarks are numbered, and different kinds of plates are indicated by letters: d, deltoid; a, ambulacral; r, radial (with A, B, and E denoting different radials); ab, azygous (unfused) basal; zb, zygous (fused) basal. *(a: From Bookstein et al., 1985; b: From Foote, 1991)*

Box 2.1

CENTROID SIZE AND SHAPE COORDINATES

Figure 2.9a depicts the cranidium of the Cambrian trilobite *Crassifimbra walcotti* with a number of landmarks indicated. These landmarks were chosen to give relatively uniform coverage to the cranidium. In this case, only landmarks on the midline and the right side are recorded. It is implicitly assumed that the form is bilaterally symmetrical—in other words, that deviations from perfect symmetry can be ignored because they are small. This example is typical in projecting the specimen into two dimensions and disregarding the third dimension for simplicity.

There are n landmarks with coordinates $(x_1, y_1), \ldots (x_n, y_n)$. The mean x- and y-coordinates are calculated as $\bar{x} = \sum_{i=1}^{n} x_i/n$ and $\bar{y} = \sum_{i=1}^{n} y_i/n$, and the centroid is defined as the point having coordinates $(\bar{x}, \bar{y})$ (see Box 3.1). The centroid size is defined as the square root of the sum of squared differences between the observed points and the centroid:

$$\text{CS} = \sqrt{\sum_{i=1}^{n} (x_i - \bar{x})^2 + (y_i - \bar{y})^2}$$

Shape coordinates can be calculated from the landmarks of Figure 2.9a by a suitable choice of scaling, shown in Figures 2.9b and 2.10. A pair of points, typically approximating the long axis of the specimen, is used to define a **baseline.** This means that one point of the baseline will become the origin in a new coordinate system, and the other baseline point will be placed on the x axis. Each additional point is treated as the vertex (point C) of a triangle, the other two vertices (points A and B) of which are the baseline points. The coordinates of these points are denoted (x_A, y_A), (x_B, y_B), and (x_C, y_C). The stored image of the specimen is then expanded or contracted so

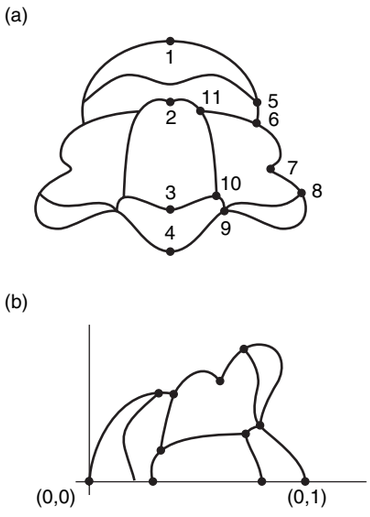

FIGURE 2.9 Orientation of a specimen for the calculation of shape coordinates. (a) Cranidium of the Cambrian trilobite *Crassifimbra walcotti*, showing a number of landmarks on the midline and right side. (b) Translation and scaling of this specimen so that points 1 and 4 define a baseline from (0, 0) to (0, 1). *(From Smith, 1998)*

The dashed lines in Figure 2.8a show distances between landmarks that can be used as measures of size. The coordinates of landmarks are commonly combined in a single size measure called **centroid size,** based on the distances of each point from the centroid or arithmetic mean of all points (Bookstein, 1991) (Box 2.1). The landmarks may also be converted to shape measures called **shape coordinates** (see Figures 2.9 and 2.10 in Box 2.1). If the landmarks are well chosen, they can provide a representation of the form that includes many aspects of shape.

Many organisms have prominent shape features that are characterized neither by a geometric model such as the logarithmic spiral nor by a set of landmarks. Consider the living mussel *Mytilus edulis*, shown in Figure 2.11. The shape of its outline would not be approximated well by a model such as a rectangle. Moreover, although we could select a number of points on the outline, their biological equivalence among specimens would not be evident; they would not be landmarks such as those in the examples of Figures 2.8 and 2.9.

In cases like that of the mussel outline, we can take advantage of methods of curve fitting. One of the most common is harmonic analysis (Box 2.2). Its utility stems from the fact that any simple curve can be described mathematically as the sum of a series of sine and cosine curves, each one multiplied by a different number called the *harmonic coefficient*. The particular values of the harmonic coefficients depend on the shape of the curve.

that the origin point of the baseline has coordinates (0, 0) and the other baseline point has coordinates (1, 0). Thus, the baseline is given a length of 1 unit. This scaling is done in such a way that the *relative* positions of the points are unaffected, that is, so that the shape of the specimen is not changed. The three points of the triangle are now denoted A′, B′, and C′. The x- and y-coordinates of point C′ summarize all the shape information that is contained in the triangle. These coordinates are obtained by the following formulas that come from trigonometry:

$$x_{C'} = \frac{(x_B - x_A)(x_C - x_A) + (y_B - y_A)(y_C - y_A)}{(x_B - x_A)^2 + (y_B - y_A)^2}$$

and

$$y_{C'} = \frac{(x_B - x_A)(y_C - y_A) - (y_B - y_A)(x_C - x_A)}{(x_B - x_A)^2 + (y_B - y_A)^2}$$

The shape coordinates are calculated in the same way for each point, and the entire set of shape coordinates gives the shape information that is present in the chosen landmarks.

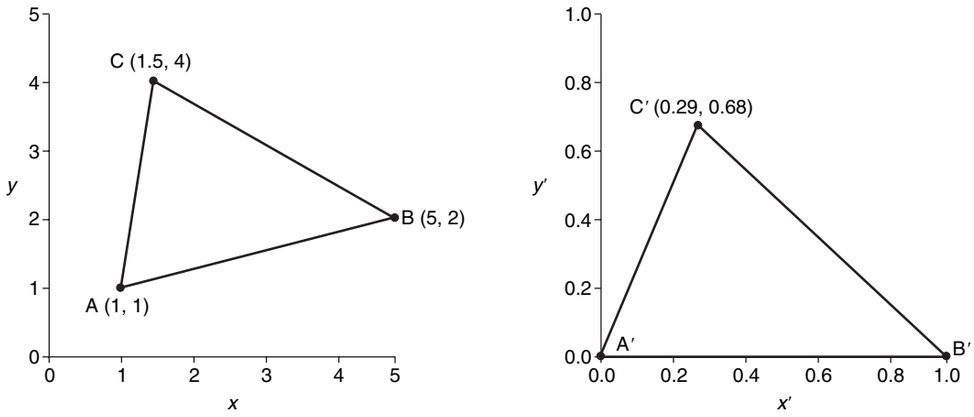

FIGURE 2.10 Transformation of hypothetical, original coordinates (left) into shape coordinates (right). Points labeled A and B are the baseline points, and point C is any other landmark. Numbers in parentheses are the x- and y-coordinates before and after transformation.

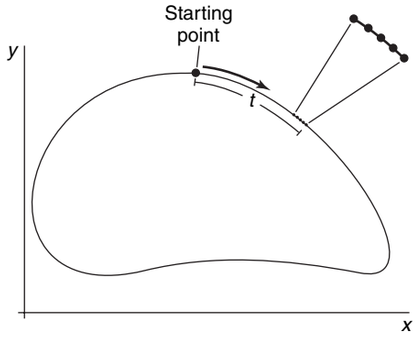

FIGURE 2.11 Outline of a specimen of the mussel *Mytilus*. Inset shows magnification of part of the outline with sampled points. The length along the curve from the starting point is given by t; the arrow shows the direction in which the curve is traced. In harmonic analysis, the x- and y-coordinates are analyzed as functions of t. *(After Ferson et al., 1985)*

In Figure 2.11, the outline of the mussel is digitized from a starting point and is represented by hundreds of stored points. Thus, it is in fact represented by a polygon—but one with so many vertices that, practically speaking, it is indistinguishable from a smooth curve. For each point, the x- and y-coordinates are recorded. The variation in x-coordinates and the variation in y-coordinates are treated as two distinct functions that depend on the length traversed along the curve from the starting point. Each function is described by a distinct set of harmonic coefficients.

Once the harmonic coefficients are calculated, the curve can be approximated by a subset of them, as shown in Figure 2.12. Clearly the outline corresponding

Box 2.2

HARMONIC ANALYSIS

Description of the outline in Figure 2.11 uses harmonic analysis, a standard approach for studying many kinds of curves. Here we describe the steps involved in one method of harmonic analysis, and we apply the approach to a simple example.

Consider the data of Figure 2.13a, which depict hourly temperature readings for five years at a weather station in Farmingdale, New York. Annual variation in temperature is clearly visible as the low-frequency (long-wavelength) oscillation. Superimposed on this annual cycle is considerable variation whose source is not immediately evident.

In this analysis, time is treated as an independent variable and temperature as a dependent variable. It is essential that the dependent variable be a single-valued function of the independent variable. In other words, for every time there is exactly one temperature. Note that the converse is not true; for any given temperature, there may be numerous times that correspond to that reading. In the data of Figure 2.13, temperature is recorded at evenly spaced (hourly) intervals. The approach to harmonic analysis presented here assumes evenly spaced values of the independent variable, in this case, time.

The general harmonic equation has the form:

$$T = \sum_{k=0}^{\infty} A_k \cos(k\Theta) + B_k \sin(k\Theta)$$

This says that the function T (here, temperature) can be expressed as the sum of an infinite number of periodic cosine and sine curves. The numbers A_k and B_k are the harmonic coefficients, the numbers by which the ideal cosine and sine curves are multiplied. The harmonic number k refers to the period of the cosine and sine curves. For example, $k = 1$ implies a curve that repeats once within the total span of time; $k = 2$ implies a curve that repeats twice; and so on. Thus, higher harmonic numbers correspond to finer-scale variations—those with higher frequency or shorter wavelength. With finite data, it is not possible to calculate an infinite series of harmonics. If there are n observations, the maximum harmonic number is no greater than $n/2$.

We place the n observed values of temperature in sequence and denote them by T_i, where $i = 1, \ldots, n$. The harmonic coefficients A_k and B_k are calculated for each value of k as:

$$A_k = \frac{2}{n} \sum_{i=1}^{n} T_i \cos(2\pi ik/n)$$

and

$$B_k = \frac{2}{n} \sum_{i=1}^{n} T_i \sin(2\pi ik/n)$$

These equations implicitly scale the total span of time to vary from 0 to 2π, the fundamental repeat length for a periodic function with harmonic number $k = 1$. For each harmonic, the height of the wave form—its amplitude—is given by $\sqrt{(A_k^2 + B_k^2)}$, and the power is given by $(A_k^2 + B_k^2)/2$. The higher the power, the more information on variation in the data accounted for by the corresponding harmonic.

In the temperature data of Figure 2.13a, there are 1826 days (four years of 365 days plus one leap year of 366 days), and thus $n = 43{,}824$ hourly readings. The first three readings are -4.4, -5.0, and -5.0 degrees, and the last three are 1.1, 1.1, and 0.6 degrees. Applying these equations to the first harmonic we have:

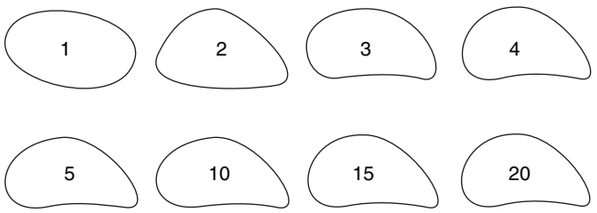

FIGURE 2.12 Approximations to the outline of *Mytilus* using different numbers of harmonics. The approximation to the outline of Figure 2.11 improves as more harmonics are included. *(From Ferson et al., 1985)*

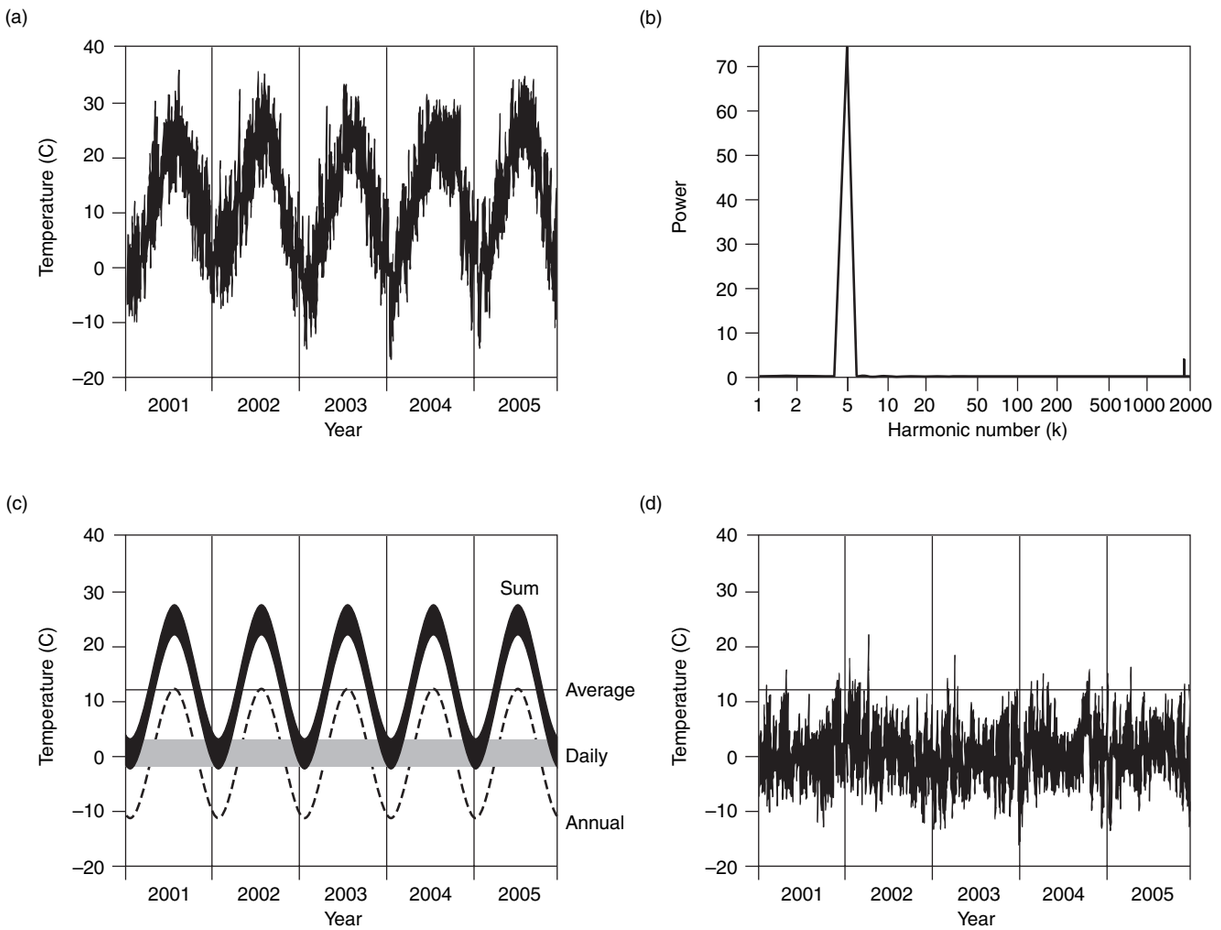

FIGURE 2.13 Harmonic analysis of temperature data. (a) Temperature in degrees centigrade, taken at hourly intervals for five years at Republic Airport, Farmingdale, New York. Missing readings are replaced by data from nearby weather stations. (b) Power spectrum, showing peaks at harmonics 5 and 1826, corresponding to annual and daily cycles. (c) Reconstructed temperature based on annual harmonic (dashed line), daily harmonic (gray band), overall average (horizontal line), and the sum of these three components (dark band). (d) Residual temperature variation (variation not accounted for by average, annual, and daily terms), calculated as the difference between the data in part (a) and the dark band in part (c). *(Data from National Oceanic and Atmospheric Administration [http://cdo.ncdc.noaa.gov/ulcd/ULCD, accessed 30 January 2006])*

continued on next page

to the first harmonic is a poor approximation to the original outline. Successively higher harmonics generally represent finer-scale aspects of the form. As more of the higher harmonics are added to the reconstruction, this reconstruction approximates the original form progressively better. Although it may not be immediately obvious that anything has been gained by the harmonic analysis, it is usually the case that a relatively small number of harmonics can provide a good approximation to the original form. Thus, the form is represented far more efficiently than would have been possible by simply recording the x- and y-coordinates of the entire outline. In the case of the mussel, hundreds of points were recorded, whereas only 20 harmonics are needed to provide the excellent approximation shown in Figure 2.12.

Box 2.2 (continued)

$$\begin{aligned} A_1 = (2/43{,}824)\{&(-4.4)\cos[2\pi(1)(\mathbf{1})/43{,}824] \\ &+ (-5.0)\cos[2\pi(2)(\mathbf{1})/43{,}824] \\ &+ (-5.0)\cos[2\pi(3)(\mathbf{1})/43{,}824] + \\ &\cdots \\ &+ (1.1)\cos[2\pi(43{,}822)(\mathbf{1})/43{,}824] \\ &+ (1.1)\cos[2\pi(43{,}823)(\mathbf{1})/43{,}824] \\ &+ (0.6)\cos[2\pi(43{,}824)(\mathbf{1})/43{,}824]\} \end{aligned}$$

and

$$\begin{aligned} B_1 = (2/43{,}824)\{&(-4.4)\sin[2\pi(1)(\mathbf{1})/43{,}824] \\ &+ (-5.0)\sin[2\pi(2)(\mathbf{1})/43{,}824] \\ &+ (-5.0)\sin[2\pi(3)(\mathbf{1})/43{,}824] + \\ &\cdots \\ &+ (1.1)\sin[2\pi(43{,}822)(\mathbf{1})/43{,}824] \\ &+ (1.1)\sin[2\pi(43{,}823)(\mathbf{1})/43{,}824] \\ &+ (0.6)\sin[2\pi(43{,}824)(\mathbf{1})/43{,}824]\} \end{aligned}$$

where the harmonic number is indicated in bold and the ellipsis (. . .) stands for the remaining readings between the first three and the last three. Similarly, for the second harmonic:

$$\begin{aligned} A_2 = (2/43{,}824)\{&(-4.4)\cos[2\pi(1)(\mathbf{2})/43{,}824] \\ &+ (-5.0)\cos[2\pi(2)(\mathbf{2})/43{,}824] \\ &+ (-5.0)\cos[2\pi(3)(\mathbf{2})/43{,}824] + \\ &\cdots \\ &+ (1.1)\cos[2\pi(43{,}822)(\mathbf{2})/43{,}824] \\ &+ (1.1)\cos[2\pi(43{,}823)(\mathbf{2})/43{,}824] \\ &+ (0.6)\cos[2\pi(43{,}824)(\mathbf{2})/43{,}824]\} \end{aligned}$$

and

$$\begin{aligned} B_2 = (2/43{,}824)\{&(-4.4)\sin[2\pi(1)(\mathbf{2})/43{,}824] \\ &+ (-5.0)\sin[2\pi(2)(\mathbf{2})/43{,}824] \\ &+ (-5.0)\sin[2\pi(3)(\mathbf{2})/43{,}824] + \\ &\cdots \\ &+ (1.1)\sin[2\pi(43{,}822)(\mathbf{2})/43{,}824] \\ &+ (1.1)\sin[2\pi(43{,}823)(\mathbf{2})/43{,}824] \\ &+ (0.6)\sin[2\pi(43{,}824)(\mathbf{2})/43{,}824]\} \end{aligned}$$

and so on for the higher harmonics.

Figure 2.13b depicts what is known as the power spectrum, a plot of power versus harmonic number k. There are two peaks in this spectrum, a large one at $k = 5$ and a smaller one at $k = 1826$. The coefficients for these two harmonics are ($A_5 = -10.8$, $B_5 = -5.5$), and ($A_{1826} = -2.0$, $B_{1826} = -1.6$).

The larger peak corresponds to a periodic function that repeats five times in five years; in other words, it is the annual cycle. The smaller peak is the daily cycle, which repeats 1826 times. If we compare the power of these two harmonics with the sum over all harmonics, we find that the annual and daily cycles account for 76.9 percent and 3.5 percent of the temperature variation for these five years. Thus, harmonic analysis allows a very efficient summary of information. Most of the information can be accounted for by just two harmonics, while less than 20 percent of the variation is spread throughout the remaining harmonics (of which there are nearly 22,000).

To reconstruct the predicted curve corresponding to a given number of harmonics, the following equation is applied:

$$\hat{T}_i = \sum_k A_k \cos(2\pi ik/n) + B_k \sin(2\pi ik/n)$$

We have summarized but a few of the available methods for morphological description. Many more are used routinely, and new ones are being developed all the time, often in fields far removed from paleontology. Historically, some of the greatest advances in paleontology have been made by those who have successfully adapted techniques from other disciplines. For example, crystallographers describe minerals with a system that includes their axes of symmetry (Figure 2.14a). Crystalline calcite in the rhombohedral habit has one principal axis of threefold rotational symmetry (termed the *c* axis) and three symmetry axes perpendicular to this (termed the *a* axes). Despite their intricate microstructure, echinoderm plates are, crystallographically speaking, single crystals of calcite. The spatial orientations of their crystal axes can be measured with equipment such as an optical goniometer,

where $\hat{T}_i$ is the predicted value corresponding to the observed value T_i, and the sum is taken only over selected values of k. For example, the predicted value of the first reading, based only on the overall average of 11.9 degrees and the annual cycle with $A_5 = -10.8$ and $B_5 = -5.5$, is equal to:

$$\hat{T}_1 = 11.9 + (-10.8)\cos[2\pi(1)(\mathbf{5})/43{,}824] + (-5.5)\sin[2\pi(1)(\mathbf{5})/43{,}824]$$

which is equal to 1.1. Thus, the observed temperature reading of −4.4 is a few degrees lower than would be predicted simply on the basis of the annual cycle. If we also added the daily cycle with $A_{1826} = -2.0$ and $B_{1826} = -1.6$, then we would have:

$$\hat{T}_1 = 11.9 + (-10.8)\cos[2\pi(1)(\mathbf{5})/43{,}824] + (-5.5)\sin[2\pi(1)(\mathbf{5})/43{,}824] + (-2.0)\cos[2\pi(1)(\mathbf{1826})/43{,}824] + (-1.6)\sin[2\pi(1)(\mathbf{1826})/43{,}824]$$

which is equal to −1.2. It makes sense that including the daily cycle leads to a lower predicted temperature, as the time in question is shortly after midnight. Even with the daily cycle taken into account, however, the reading of −4.4 is lower than expected.

Figure 2.13c shows curves corresponding to the annual and daily cycles. The daily variation is of such high frequency that it appears as a blur. The amplitude of the annual harmonic is 12.1 degrees, implying a temperature range of 24.2 degrees. This is about 5 times that of the daily harmonic, with an amplitude of 2.6 degrees. (The difference in power between annual and daily cycles is so much greater than the amplitude difference because power is proportional to the square of the amplitude.)

Superimposed on Figure 2.13c is the sum of the annual cycle, the daily cycle, and the average temperature. This combination of three terms tracks the original data reasonably well. Finally, Figure 2.13d shows the actual data with the average and the annual and daily cycles subtracted out. This is the residual variation in temperature for the recorded interval of time that is not accounted for by the average, annual, and daily terms. Weather services attempt, with occasional success, to predict the short-term pattern of residual variation in temperature that is not accounted for by simple daily and annual cycles.

For the outline of Figure 2.11, the length along the curve is treated as the independent variable, and the *x*- and *y*-coordinates are treated as two dependent variables. Two separate harmonic analyses are carried out, one for *x* and one for *y*, which result in four sets of harmonic coefficients. It may not seem obvious that this outline has a regular periodicity like the temperature data of Figure 2.13a. It must be periodic, however, because the starting and ending points are the same. In biological shapes such as that of Figure 2.11, there is often a clear relationship between the harmonic coefficients and major features of shape. An outline with strong four- or fivefold symmetry, for example, will tend to have high power in the fourth or fifth harmonics.

Harmonic analysis has many important applications in the earth sciences. For example, analysis of late Cenozoic climatic records has provided crucial empirical support for theoretical arguments that global temperature and other aspects of climate vary predictably, on timescales of tens of thousands of years, in response to variations in the earth's orbit and rotational axis. Harmonic analysis has also been used to detect cycles in biological diversity and extinction over geologic time [SEE SECTION 8.6].

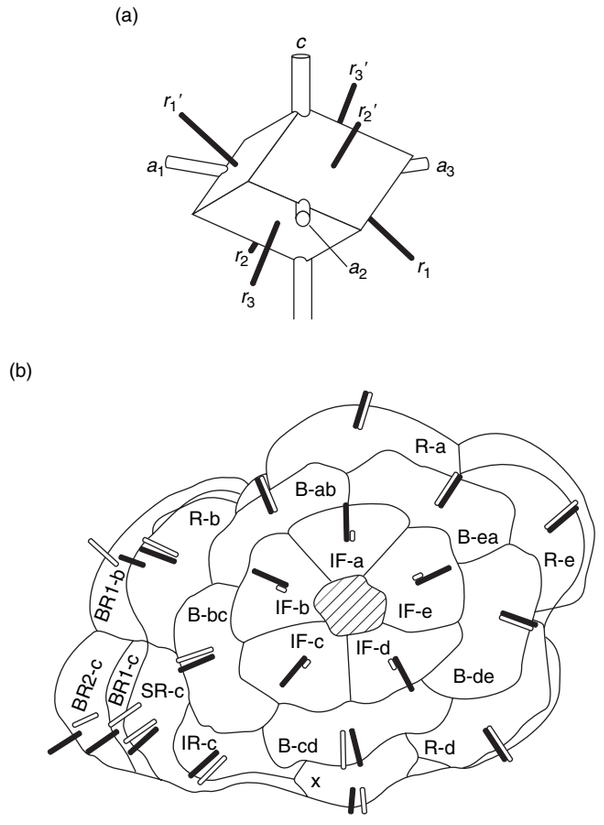

FIGURE 2.14 Crystallographic axes of a calcite crystal and orientations of axes on a crinoid. In part (a), the labels *c* and *a* indicate the *c* and *a* axes, and *r* indicates the direction that is normal to the crystal face. In part (b), the crinoid is in basal view, the lightly shaded rods indicate the direction of *c* axes, and the darker rods indicate the direction that is normal to the plate surface. Uppercase letters indicate different kinds of plates, and lowercase letters denote different positions of these plates (IF, infrabasal; B, basal; R, radial; IR, infraradial; SR, superradial; X, anal; BR, brachial). *(a: From Bodenbender, 1996; b: From Bodenbender & Ausich, 2000)*

and these axis orientations can be formally treated as shape variables.

Figure 2.14b shows typical crystallographic axis orientations in a **CRINOID** calyx. The light lines show the directions of *c*-axis orientation on a number of plates. For comparison, the dark lines indicate the directions of the vectors perpendicular to each plate surface. For many plates the two lines do not coincide; thus, the crystallographic axes provide additional information that is not present in the shape of the plate surface.

2.3 THE NATURE OF GROWTH AND DEVELOPMENT

Earlier we stated that one of the three major aspects of organic form is the relationship between size and shape. This relationship is expressed during the growth and development, or **ontogeny,** of individual organisms. Knowing how form changes with growth is often central to understanding biologic function. It is also necessary for a complete understanding of variation—for example, whether two dissimilar forms represent different species or just growth stages of the same species. Studying ontogeny is also essential to the study of evolution, because evolutionary change in adult form is effected through the evolution of ontogeny.

A special case of ontogeny is **astogeny,** the growth and development of colonial organisms. Animals such as **GRAPTOLITES, BRYOZOANS,** and corals typically consist of tens to thousands of genetically identical, **clonal,** units. They carry out life functions and in many ways resemble distinct organisms. In many cases, they can even be highly specialized to perform different functions—some dedicated to feeding, others to defense, and still others to reproduction. The soft "animal" of each unit is known as a *zooid* in graptolites and bryozoans, and as a *polyp* in corals. The corresponding skeletal unit is referred to as a *theca* in graptolites, a *zooecium* in bryozoans, and a *corallite* in corals.

The astogeny of a bryozoan colony is illustrated in Figure 2.15. The colony begins as a single zooid attached to a substrate such as a bit of shell or a rock. In this case, the zooids first proliferate horizontally to provide a base for the colony. Vertical growth then ensues, after which some zooids become thickly calcified and specialized for support, while others are dedicated to feeding and reproduction. Of course, each unit undergoes its own ontogeny in addition to being part of the astogeny of the larger colony. Because of this, and because both the single units and the colony must maintain function as they grow, colonial organisms are somewhat more complicated to study than are solitary organisms. Nevertheless, the tools used to study astogeny are the same as those used to study ontogeny.

Types of Growth

Organic growth is extremely complicated; it usually involves several types of change, among which are changes in cell size, number of cells, number of cell types, and, especially in animals, relative positions of cells. During life,

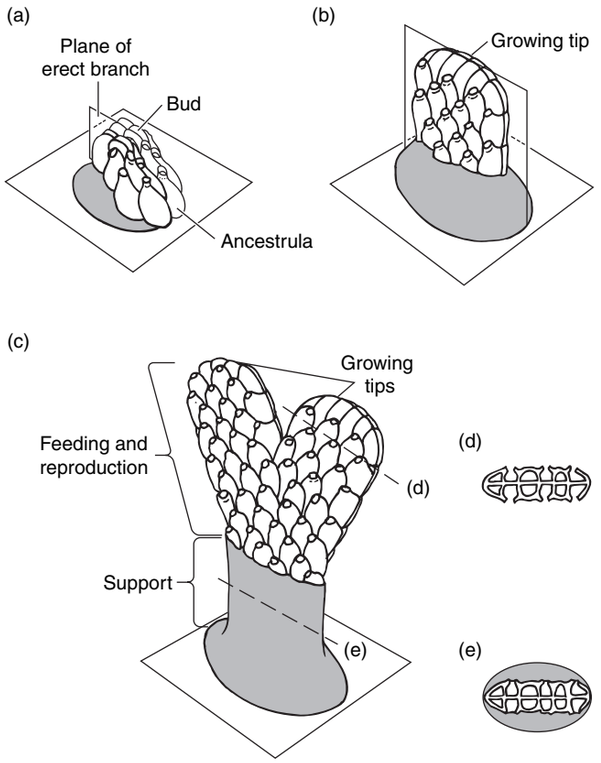

FIGURE 2.15 Idealized astogeny in a living bryozoan colony. Parts (a) through (c) show three developmental stages. The ancestrula is the founding member of the colony. A bud is a newly generated zooid. Parts (d) and (e) show cross sections through two locations at stage (c). *(From Cheetham, 1986a)*

FIGURE 2.16 Accretionary growth at apical meristems. (a) Thin section of apical meristem of a Carboniferous sphenopsid, showing a single apical cell (arrow) from which the surrounding cells divided. Magnification is ×150. (b) Schematic diagram of accretionary growth at an apical meristem. Arrows show the directions of growth. This example has a single apical cell, but many other cellular configurations are known. *(a: From Good & Taylor, 1993; b: From Fahn, 1982)*

an organism may change in form abruptly or it may change gradually. Growth, especially of hard skeletons, takes place in a few major ways and in combinations of these.

Accretion of Existing Parts Organisms in many biologic groups grow by adding new material at growth zones throughout ontogeny. For example, proliferation of new cells in vascular plants takes place at special regions called **meristems.** Apical meristems are at the growing tips and are responsible for increase in length. Figure 2.16a shows a magnified image of an apical meristem in a Carboniferous **SPHENOPSID.** A single apical cell is present, indicated by the arrow. As cells divide from the apical cell, they are pushed away from the tip, with the result that older cells are farther away. This process is illustrated schematically in Figure 2.16b, which shows the apical cell at the top; directions of accretionary growth are indicated by the arrows. In general, cells outside the meristems do not divide once they are produced, although they typically change in form to differentiate for specialized functions.

Figure 2.17 shows a cross section through the stem of a seed plant, with some tissue types indicated. Five major tissues are produced at the apical meristems: pith, xylem, phloem, cortex, and epidermis. These are referred to as primary tissues. Secondary tissues have evolved numerous times in plants. For example, in seed plants there is a layer of vascular cambium, a lateral meristem that produces secondary xylem and secondary phloem. Accretionary growth at the vascular cambium takes place in two opposite directions, resulting in a thickening of the stem. In many different kinds of plants, the epidermis is eventually shed, and the cortex and primary phloem are crushed as they are pushed

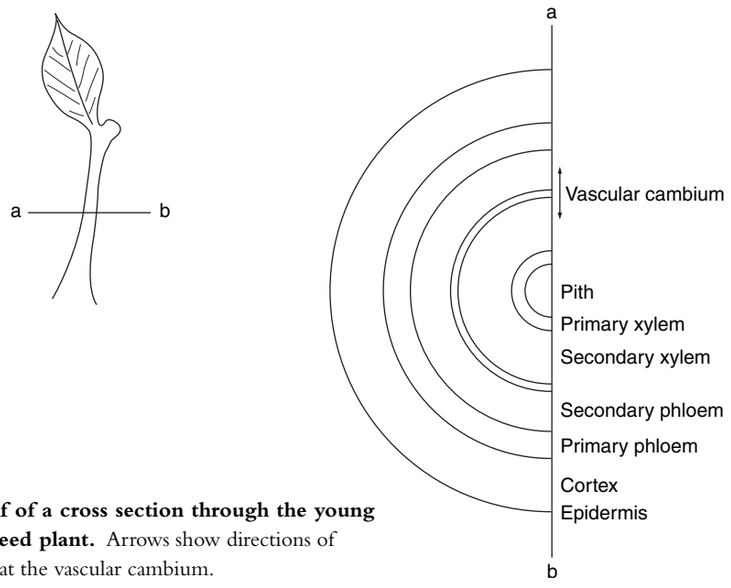

FIGURE 2.17 Half of a cross section through the young stem of a typical seed plant. Arrows show directions of accretionary growth at the vascular cambium.

outward, forming the dead outer bark. In these plants there is a secondary cortex as well.

Growth by accretion is especially common among animals whose shell is external and serves primarily for protection and muscle attachment—for example, brachiopods, gastropods, cephalopods, and bivalved molluscs. Figure 2.18 illustrates growth in a bivalve. The cross section of the shell is marked by growth lines that can be observed in the shell as well as on the outer surface. New skeletal material is added not only at the leading edge of

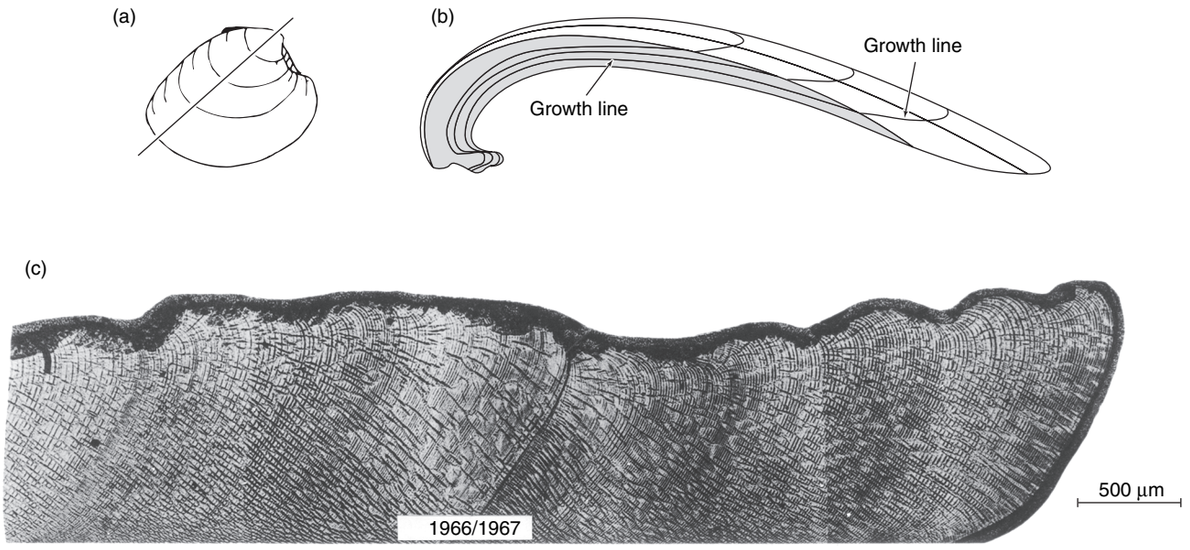

FIGURE 2.18 Accretionary growth in bivalved molluscs. (a) The exterior of one shell of the species *Mercenaria mercenaria*, with three prominent, concentric growth lines. The straight line gives the position of a section through the shell, shown in part (b). The photograph in part (c) shows approximately one year's growth in a specimen of this species. The leading edge of the shell is to the right. The dark band near the middle is an annual growth line, and the finely spaced bands that run roughly parallel to this are daily growth increments. *(From Pannella & MacClintock, 1968)*

the shell, but also as a covering over most of the interior surface of the shell. Figure 2.18 includes an enlarged photograph of a series of growth lines. In this instance, the shell was grown under controlled conditions, and it is possible to establish that the growth lines are in fact daily. The dark annual growth line, corresponding to the slowing of growth in the winter, can also be clearly seen. The ability to correlate growth lines with astronomical cycles is useful in many areas of research (see Figure 2.34 and Sections 9.5 and 10.5).

Addition of New Parts A common method of skeletal growth for those organisms whose skeletons consist of many parts, either tightly articulated or fitting loosely in the soft tissue, is addition of new skeletal parts.

Figure 2.19 schematically shows some aspects of the growth of crinoid stems by addition of new columnals. In this type of growth, large columnals are added periodically at the base of the calyx (labeled A and B in Figure 2.19). They may or may not grow appreciably by accretion after their formation. As each new columnal is added at the calyx, the previous ones are displaced down the stem. At some distance away from the calyx, smaller columnals appear between the preexisting ones. They grow by accretion and, as they do, still more small columnals are intercalated. The result of this process (labeled E in Figure 2.19) is an orderly set of generations of intercalated columnals—with the generations being distinguishable by size.

Addition of new parts is integral to the growth of many other organisms. Figure 2.20 shows several stages in the ontogeny of a trilobite. One of the more obvious ontogenetic changes is the gradual addition of segments.

Molting Like other arthropods, the trilobite shown in Figure 2.20 used another basic mechanism of growth, the periodic shedding or molting of the entire skeleton and formation of a new one to accommodate the increase in size of the soft parts. Figure 2.21 shows a plot of head width against length in an assemblage of the Middle Ordovician trilobite *Trinodus elspethi*. The measurements fall into clusters, each representing a molt stage, between which size increases in steps. Differences between points in a cluster represent minor differences in size and shape among the individuals of that stage.

Modification In many groups, skeletal material is continually resorbed and redeposited as the skeleton grows.

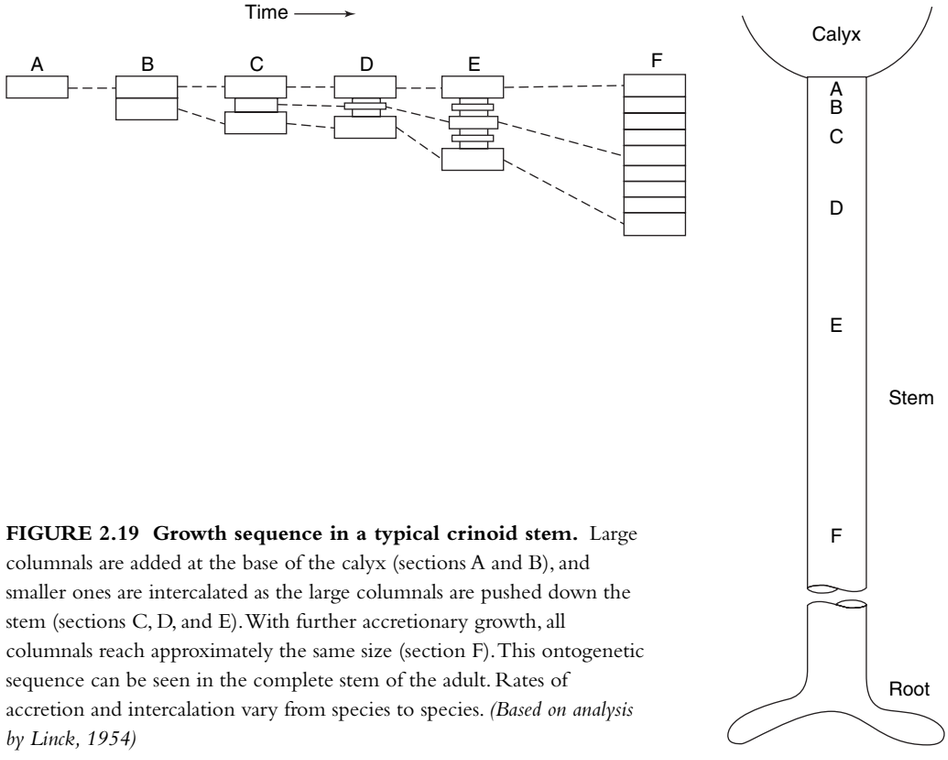

FIGURE 2.19 Growth sequence in a typical crinoid stem. Large columnals are added at the base of the calyx (sections A and B), and smaller ones are intercalated as the large columnals are pushed down the stem (sections C, D, and E). With further accretionary growth, all columnals reach approximately the same size (section F). This ontogenetic sequence can be seen in the complete stem of the adult. Rates of accretion and intercalation vary from species to species. *(Based on analysis by Linck, 1954)*

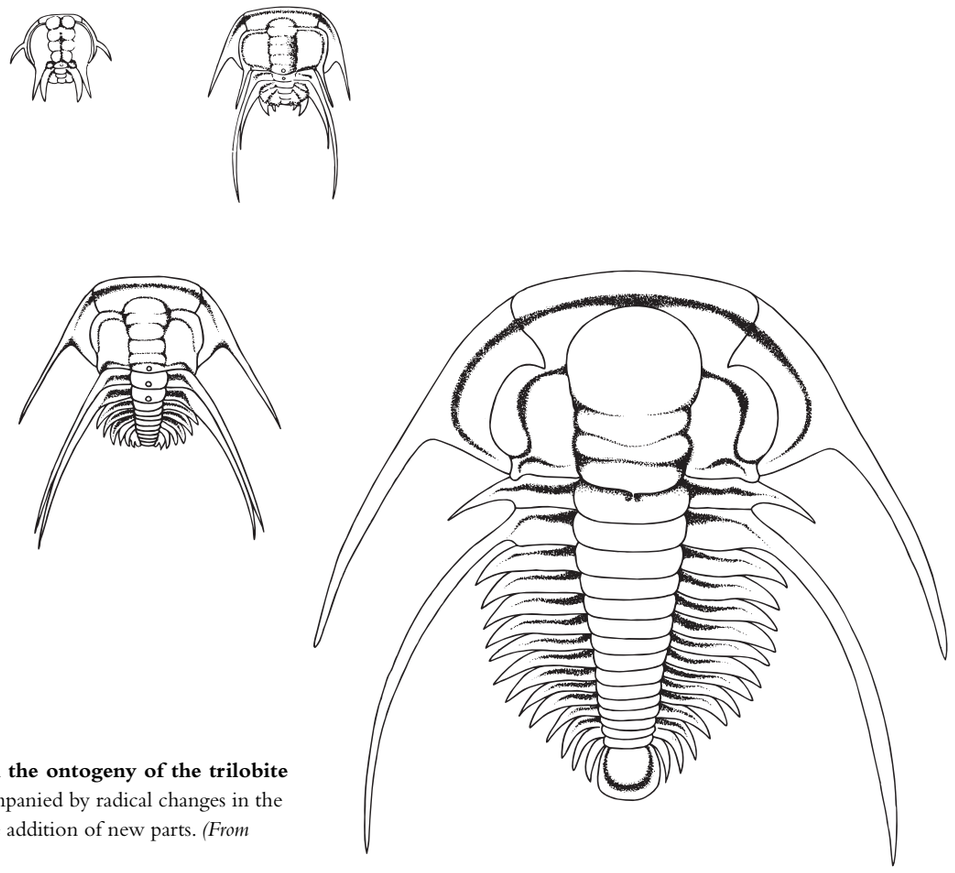

FIGURE 2.20 Four stages in the ontogeny of the trilobite *Paradoxides*. Ontogeny is accompanied by radical changes in the form of existing parts and by the addition of new parts. *(From Whittington, 1957)*

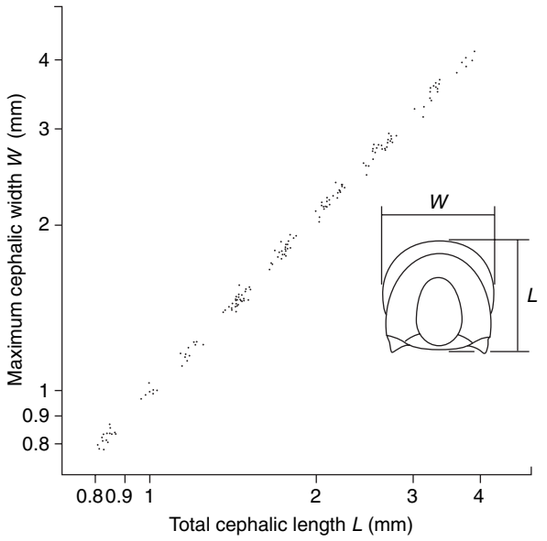

FIGURE 2.21 The ontogeny of the head of the Ordovician trilobite *Trinodus* as measured by the development of length and width dimensions. Clusters reflect molt stages, with the major increase in size taking place from one stage to the next. *(From Hunt, 1967)*

The result is that the entire form of the skeleton changes, not just a well-defined growing margin. Growth by modification is common in the bones of vertebrates (Figure 2.22), but it also occurs in organisms otherwise typified by accretionary growth, such as certain molluscs and echinoderms.

The modes of growth just outlined are idealized end-members. Many organisms in fact grow by a combination of these modes. The crinoid stem (Figure 2.19) combines addition of new parts and accretion of existing parts, and the trilobite (Figure 2.20) combines molting and addition of parts.

Describing Ontogenetic Change

In living organisms we can observe growth as it occurs. Therefore, ontogenetic changes can be studied in detail, and the timing of changes can be determined. With fossil material, as with specimens of living forms in which growth has already taken place, ontogenetic change and its

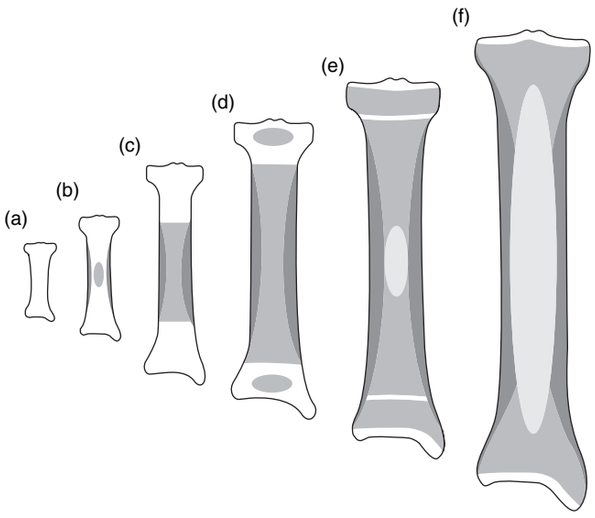

FIGURE 2.22 Growth of a mammalian limb bone by modification. (a) Initial deposition of nonmineralized cartilage (white). (b) Early replacement of cartilage by spongy bone (medium gray). (c, d) Further deposition of spongy bone and replacement of some spongy bone by compact bone (dark gray). (e) Formation of marrow (light gray) and continued modification of bone. (f) Expansion of marrow and continued bone modification. At this point, only the ends of the bone are cartilage. *(From Romer, 1970)*

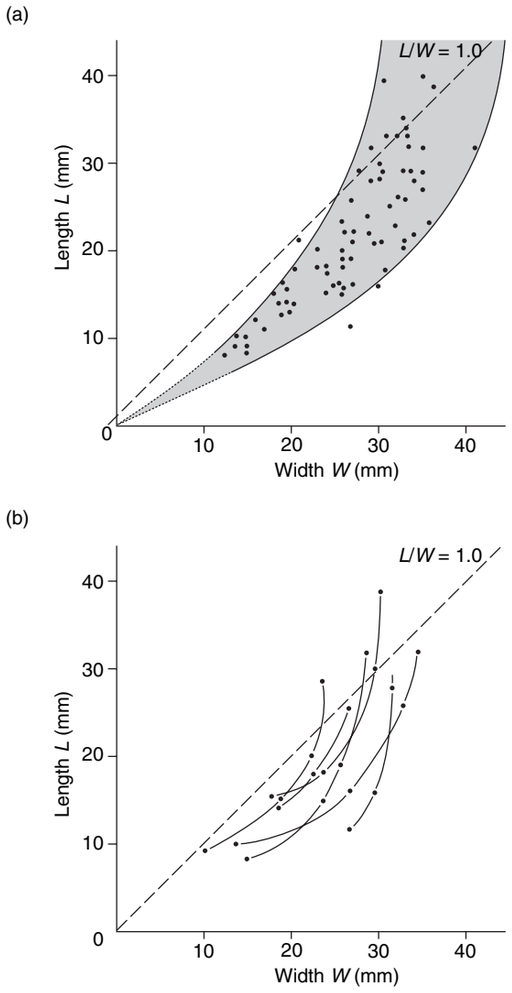

FIGURE 2.23 Ontogenetic change in shape in brachiopods. Plots are of measurements made on an assemblage of the Carboniferous brachiopod *Ectochoristites*. Length refers to the anteroposterior (front-to-back) length of the pedicle valve; width is measured along the hinge of the pedicle valve. Points connected by curved lines in the lower graph are based on growth-line measurements of single specimens. *(From Campbell, 1957)*

timing cannot be directly observed. There are two general approaches to studying ontogeny in fossils, **cross-sectional analysis** and **longitudinal analysis.**

In cross-sectional studies, a series of specimens at different sizes or growth stages is compared to study change in shape with increasing size. Because the growth of individual organisms is not followed, this is an approximate procedure. It is generally the only one available with fossils, however.

In longitudinal analysis, the ontogeny of a single organism is followed. With fossils, of course, this is possible only for organisms that keep a record of their growth. For example, the bivalve of Figure 2.18 is an adult, but its growth lines show the form of the margin at various times throughout its life. Its ontogeny is recorded in its adult shell. In general, longitudinal analysis of fossils can be applied only to organisms that grow by simple accretion at a margin and that do not radically modify the skeleton once it is laid down. For reconstructing ontogeny, longitudinal analysis is more direct than cross-sectional analysis and is therefore generally preferable if it can be carried out.

It is worth asking how well a cross-sectional analysis can approximate ontogenetic change. Figure 2.23 depicts the length and width of a number of shells of a brachiopod species. Figure 2.23a shows a cross-sectional analysis; each point is a distinct individual of a different size collected from the same assemblage. The scatter of points suggests a curved growth trajectory. Smaller shells are below the 45° line that marks equal length and width; they are wider than long. Larger shells are above this line; they are longer than

wide. But the curved scatter of points does not necessarily imply that the growth trajectories of individual shells were also curved. In a cross-sectional study such as this, we assume that individual growth roughly follows that of the average curve. In this case, we can test the assumption directly, because the brachiopods grew by accretion. Each growth curve shown in Figure 2.23b was reconstructed by measuring a single adult shell at a series of points corresponding to growth lines. In this case, the longitudinal analysis confirms the suggestion of the cross-sectional study—that the individual growth pattern in this species was curved.

A different approach to describing ontogenies of entire organisms or parts of them is to use **coordinate transformation,** a method that also has been adapted to describe differences between individuals in a population and even between related species. This approach was first suggested by D'Arcy Wentworth Thompson in his classic work *On Growth and Form*. Since that time, several mathematical descriptions of coordinate transformation have been developed.

Perhaps the most promising of these is the method of the **thin-plate spline.** (A spline is simply a mathematical function that interpolates smoothly between points; it approximates the position of intermediate values between observed points. Physical splines, made of flexible wood, are used in graphic design to draw curves.) The two forms to be compared must have a set of corresponding landmarks whose x- and y-coordinates are recorded, as described earlier in this chapter. The deformation of one form to the other—the changes in the x- and y-directions that must be added to each of the landmarks of the first form in order to produce the second form—can be described as a combination of a few well-characterized mathematical functions. As with the sine and cosine functions used in harmonic analysis, the functions of the thin-plate spline are quite general; they take on different coefficients depending on the two forms being compared. The deformations are defined not only at the landmarks; as the name of the spline method suggests, they are also interpolated between points.

Figure 2.24 illustrates the thin-plate spline approach applied to growth in the Lower Cambrian trilobite *Olenellus fowleri*. Figure 2.24a is a photograph of a juvenile specimen with the positions of a number of landmarks indicated. The landmarks on this same specimen are shown on a grid in Figure 2.24b, and the positions of the corresponding points on an adult are shown in Figure 2.24c. Comparing the juvenile and adult landmarks, there are two prominent features of shape change through ontogeny. First is an inflation of the glabella, the central region of the head marked by points 3–16. Second is a lateral movement of the genal spines, marked by points 17, 19, and 21 on the left and by 18, 20, and 22 on the right. Figure 2.24d depicts the grid deformation involved in the shift of landmarks between juvenile and adult. The dilation of the grid near the center corresponds with the glabellar inflation, and the stretching of the posterior margin of the grid corresponds with the movement of the genal spines.

Growth Rates

Some plants and animals grow very rapidly; others grow very slowly. About 20 years are generally required, for example, to complete human growth. Other organisms, such as insects, may go through a complete ontogeny in a matter of days or weeks. In nearly all organisms, the rate of growth varies with time; that is, it changes during ontogeny. One of the principal differences between organisms lies in whether growth eventually ceases. In organisms with **determinate growth,** such as most **MAMMALS,** a mature stage is reached in which structural growth stops even though the organism continues to live. (Humans show determinate growth, even though it is common to put on weight later in life.) In most plants and animals, however, growth is **indeterminate,** continuing throughout the life of the organism but at a greatly reduced rate, making it difficult to define a true adult stage. At best we can define a stage at which most of the growth will have taken place, but growth will not have ceased.

Different parts of an organism typically grow at different rates. We have already seen an example of this in brachiopods (Figure 2.23), in which length and width grew at different rates.

Nearly all paleontologic studies of ontogeny involve the measurement of change in one morphologic attribute in relation to change in another. We can define two basically different types of growth: **isometric** growth and **anisometric** growth. If the ratio between the sizes of two parts of an organism does not change during ontogeny, we have isometric

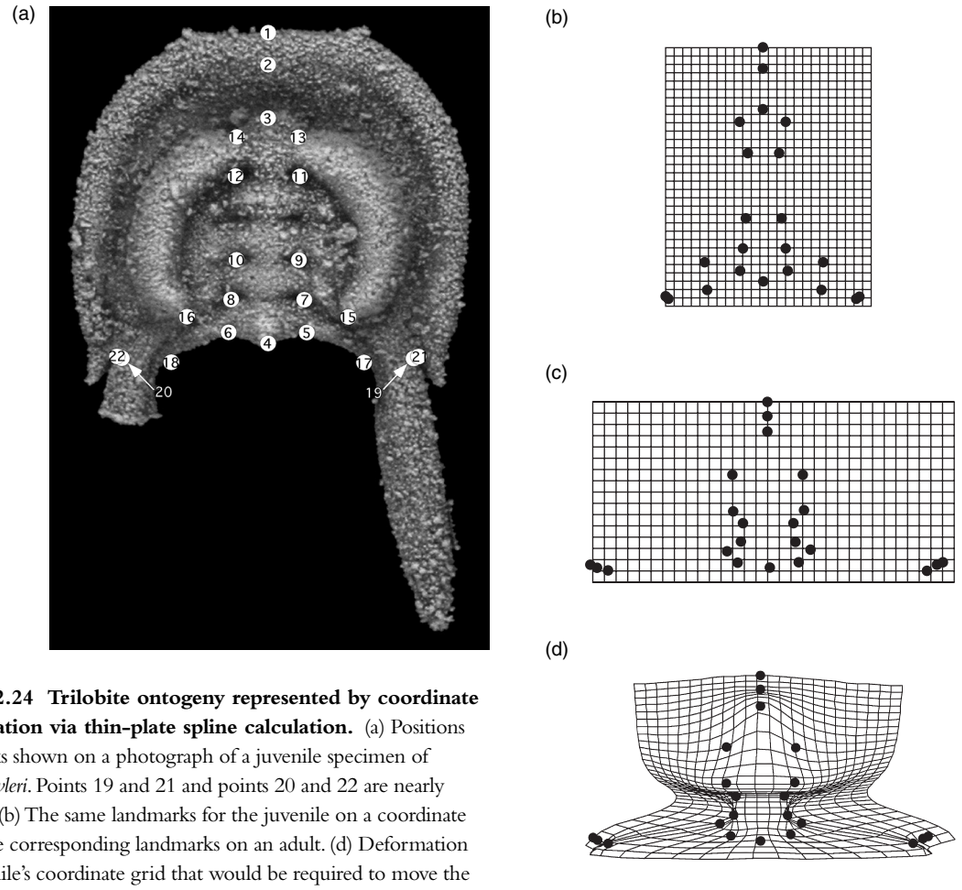

FIGURE 2.24 Trilobite ontogeny represented by coordinate transformation via thin-plate spline calculation. (a) Positions of landmarks shown on a photograph of a juvenile specimen of *Olenellus fowleri*. Points 19 and 21 and points 20 and 22 are nearly coincident. (b) The same landmarks for the juvenile on a coordinate grid. (c) The corresponding landmarks on an adult. (d) Deformation of the juvenile's coordinate grid that would be required to move the landmarks to their positions in the adult. Anterior is toward the top in (a) through (d). *(Courtesy of Mark Webster)*

growth; shape does not change as size increases (Figures 2.25a and 2.25b). If the ratio does change, we have anisometric growth; shape changes as size increases (Figures 2.25c and 2.25d). Anisometric growth is far more common than isometric growth. In other words, shape change during ontogeny is the rule rather than the exception.

Two kinds of isometric growth are shown in Figure 2.25. In the pattern of isometric growth plotted on graph (a), both parts grow at precisely the same rate. This yields a straight line at 45° to either axis. In the pattern of isometric growth plotted on graph (b), one part grows more rapidly than the other, but the ratio between them is constant. This results in a straight line that is separated from one axis by a smaller angle than from the other. In the pattern of anisometric growth plotted on graph (c), the *X* part grows more rapidly than the *Y* part at first, but this relationship is subsequently reversed. The plot of growth is a curve. The pattern of growth plotted on graph (d) is different from the other three patterns in that the plotted line would not pass through the origin if extended. In pattern (d) as in pattern (c), shape changes with growth. To summarize, growth is isometric if the plotted line is straight and passes through the origin (or would do so if extended). All other conditions produce anisometric growth.

When growth rates are expressed in absolute terms such as centimeters per year, larger dimensions generally increase more rapidly than do smaller dimensions. For example, the length of a femur may increase by 1 cm during the same span of time in which the width increases by only a few millimeters. It is therefore useful to consider **size-specific growth rates** (also known as

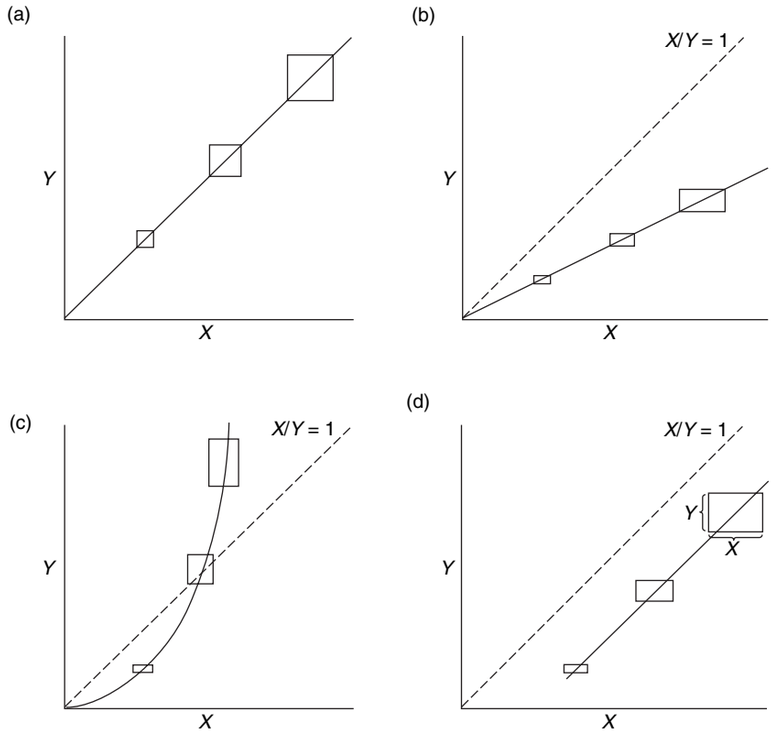

FIGURE 2.25 Typical patterns of growth observed when two morphologic dimensions are plotted against each other. In each graph, the shape of a hypothetical organism is shown by a square or rectangle at three ontogenetic stages. In parts (a) and (b), growth is isometric; there is no change in shape. In parts (c) and (d), growth is anisometric; shape is continually changing.

relative growth rates). A femur that grows in length from 10 to 11 cm in a year would have a size-specific growth rate of 1 cm per 10 cm per year, or 10 percent per year, in its length.

It is generally difficult to obtain measures of absolute age for growth stages of fossils. If we simply want to know whether two parts grew at the same size-specific rate, however, the time component cancels out when we take the ratio of relative rates. If femur length increases from 10 to 11 cm while femur width increases from 1 to 1.2 cm, the ratio of the two size-specific growth rates is 10 to 20 percent, or 1:2, even if we do not know how much time has elapsed between the smaller and larger size. Thus, it is possible to determine whether growth is isometric or anisometric, even if we cannot measure growth rates with respect to actual time. This, of course, is exactly what we saw in Figure 2.25.

Reasons for Anisometric Growth

The two principal reasons why it may be advantageous for organisms to change shape as they grow are exactly opposite each other: either to change function or to maintain function.

Consider the metamorphosis of a frog, which develops into an adult through a succession of fairly gradual changes. The tadpole lives in and depends upon an aquatic environment: It extracts oxygen directly from the water. The adult frog, although partially dependent upon the proximity of water, is essentially a terrestrial organism. Some ontogenetic changes in frog anatomy are produced by the addition of new structures and the deletion of old; others are brought about by changes in relative rates of growth. The striking differences between a tadpole and an adult frog largely reflect differences in function.

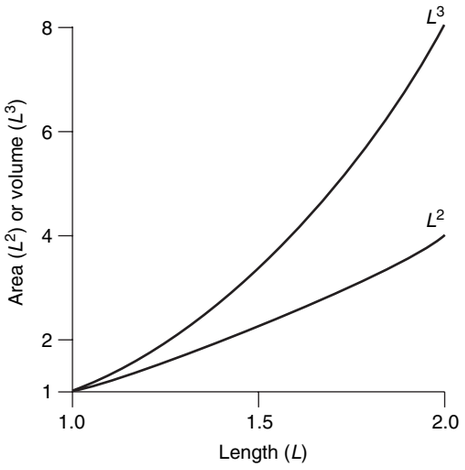

FIGURE 2.26 Effect of isometric growth in linear dimensions (L) on area (L^2) and volume (L^3). If growth is isometric, volume increases much more rapidly than does area.

Many organisms do not change function as radically as the frog does, yet they still change in shape substantially as they grow. The major reason is that, as size increases, it would not be possible to maintain function without a change in shape.

Consider a leg bone of a terrestrial vertebrate. The bone serves several functions, but one of the most important is to support the body. The strength of a bone (or any other supporting structure, for that matter) is approximately proportional to its cross-sectional area. Thus, a stout bone will be stronger than a slender bone regardless of its length. Now imagine that the entire organism grew isometrically (Figure 2.26), so that every linear dimension increased by the same proportional amount. For example, suppose every linear dimension doubled. In this case, the volume or mass (L^3) would increase eightfold $(2 \times 2 \times 2 = 8)$, but the cross-sectional area (L^2) would increase only fourfold $(2 \times 2 = 4)$. Thus, if growth were isometric, body mass would increase more rapidly than the cross-sectional area of the bone, and the bone would not be able to support the animal without breaking.

D'Arcy Thompson named this rule of scaling inequality the **principle of similitude.** To overcome such scaling problems, it is necessary for the shape of the bone to change with size. That is, the bone must become relatively stouter to carry the increased weight of the body. This is in fact what occurs in the ontogenetic development of many terrestrial vertebrates.

The principles of scaling that dictate anisometric change through growth in a single species also apply to size-related differences among species. Figure 2.27 shows the femurs of three species of pelycosaurian **REPTILES.** These are drawn at different scales; the one on the left is the longest and the one on the right is the shortest. Clearly, the longer the femur, the stouter it is. This is exactly what we would expect, given scaling of body mass and cross-sectional area.

Similar scaling principles have been deduced for many other structures as well. For example, the amount of gas that can be exchanged by a respiratory structure depends on the structure's surface area. The amount of gas exchange required by the organism depends roughly on the organism's mass or volume. Isometric growth would lead to an ever-decreasing surface:volume ratio, which would be functionally inadequate. Thus, respiratory structures in many organisms become more convoluted during growth so that respiratory surface area can keep up with body volume.

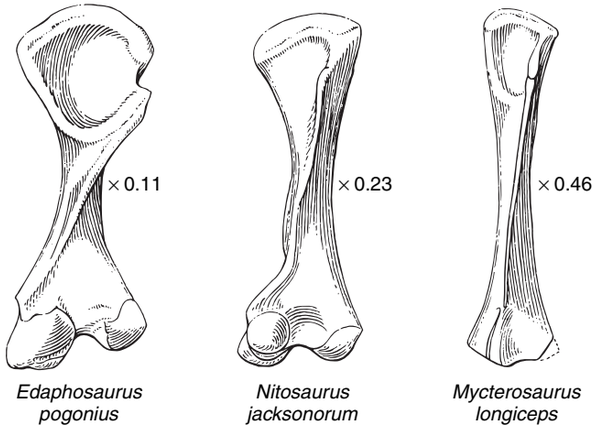

FIGURE 2.27 Femurs of three pelycosaurian reptiles, illustrating variation in proportions with increasing size. Actual size increases from right to left. Thus, longer bones are also stouter. *(From Gould, 1967)*

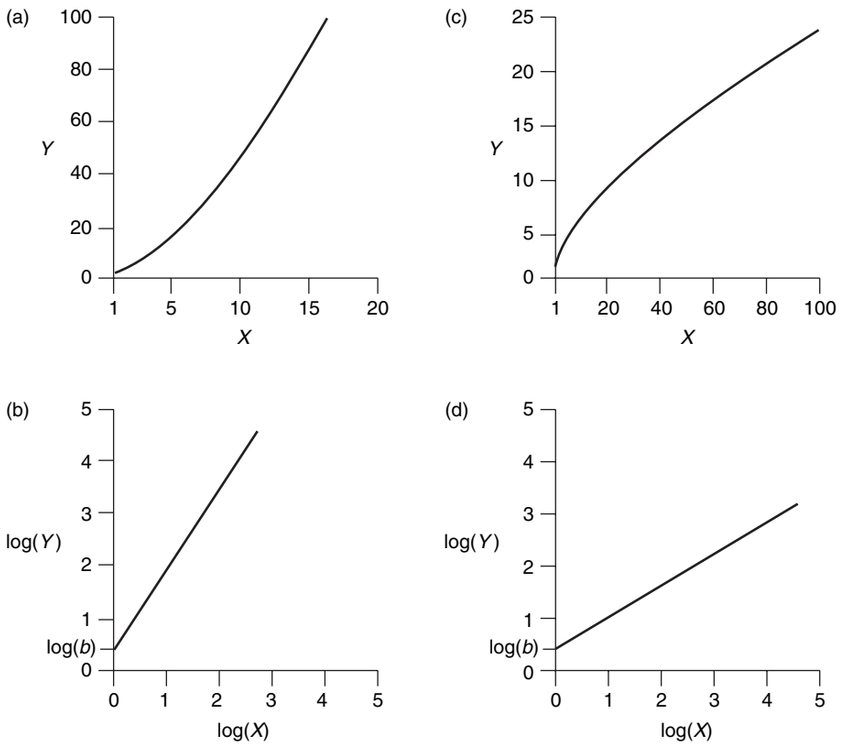

FIGURE 2.28 Patterns of allometric growth in two morphologic dimensions. Left-hand panels show positive allometry, in which *Y* grows at a higher relative rate than *X*. Right-hand panels show negative allometry.

Allometric Growth

The principle of similitude leads us to expect the prevalence of a special case of anisometric growth known as **allometry.** If *X* and *Y* are two size measures, then the general allometric equation is given by:

$$Y = bX^a$$

where *a* and *b* are constants. This equation is closely related to the size-specific rates we discussed earlier. If the growth of *X* and *Y* follows a simple form of scaling that we would expect under the principle of similitude, such as an area-to-volume relationship, then the ratio of size-specific growth rates should be constant during ontogeny; and growth will follow this equation. In fact, growth of this form is quite common. The constants *a* and *b* need to be estimated with measurement data, as shown in Figure 2.29. This is easily done with line-fitting methods [SEE SECTION 3.2]; thus, it is convenient to use an equivalent, linearized form of the allometric equation by taking the logarithm of both sides:

$$\log(Y) = a \log(X) + \log(b)$$

Although some workers use the terms *anisometry* and *allometry* interchangeably, for many purposes it is useful to recognize a distinct concept of allometry as defined here because of its simple, special, and broadly applicable formulation. Note that Figure 2.25d illustrated an example of anisometry that is not strictly allometric.

Figure 2.28 illustrates two cases of allometric growth of a trait *Y* relative to a trait *X*. In part (a), the traits are plotted on an arithmetic scale. Clearly, *Y* increases at a higher relative growth rate than *X*; *Y* is said to exhibit **positive allometry** relative to *X*. The growth relationship is curved, with the curve becoming ever steeper as size increases. Part (b) shows the same growth relationship, this time with both variables plotted on a logarithmic

scale. The relationship is now linear, and the slope of growth curve *a* is greater than 1.

Parts (c) and (d) show an example of **negative allometry,** in which *Y* increases at a lower relative growth rate than *X*. Plotted arithmetically, the growth curve becomes ever shallower as size increases. Plotted logarithmically, the growth curve is linear with a slope less than 1. Note that in both logarithmic plots, $\log(Y)$ takes on the value of $\log(b)$ when $\log(X) = 0$, that is, when $X = 1$.

We have focused so far on describing patterns of growth. An understanding of the principles underlying allometric growth can be used to test specific hypotheses about scaling as it relates to organismal function. Box 2.3 illustrates this approach with a case study.

Other Allometric Relationships

The principles of allometry that we have applied to ontogeny often help us to interpret size–shape relationships at other scales—for example, the comparison among numerous species.

Box 2.3

TESTING AN ALLOMETRIC HYPOTHESIS WITH AN ORDOVICIAN ECHINODERM

In the example that follows, measurements were taken to determine whether growth agrees with the expectations of a simple area:volume relationship. An unexpected result in this case has contributed to a better understanding of function.

Figure 2.29 shows a specimen of the **RHOMBIFERAN** echinoderm *Pleurocystites* from the Ordovician of the north-central United States. Several specialized structures known as *pectinirhombs* are circled in the photograph. These structures, which are common in rhombiferans, have a folded surface that suggests a respiratory function, and this interpretation seems quite reasonable. The respiratory function makes a clear prediction about allometric scaling. Assume that the amount of oxygen supplied to the body, or theca, is proportional to the total area of the pectinirhombs on an individual, while the amount of oxygen needed is proportional to the volume of the theca. Then we would expect the size-specific growth rate of rhomb length (L_R) to be greater than that of thecal length (L_T). Specifically, rhomb area increases only as $(L_R)^2$, while thecal volume increases as $(L_T)^3$. For rhomb area to increase in growth as rapidly as thecal volume does, L_R would have to increase in proportion to L_T raised to exponent 3/2, or 1.5. Because $[(L_R)^{3/2}]^2 = (L_R)^3$, such a scaling would allow thecal area to keep up with thecal volume. Thus, we would expect a logarithmic plot of rhomb length against thecal length to have a slope of 1.5. This is the same as saying a logarithmic plot of rhomb area against thecal volume should have a slope of 1.0.

The comparison between respiratory area and thecal volume is depicted in Figure 2.29b, showing a cross-sectional analysis in which each point is a measured individual of a different size. Rhomb area increases even more rapidly than is required by the simple scaling relationship; the double log plot of rhomb area against thecal volume has a slope of 1.3 rather than the expected 1.0. This suggests that some unknown factor limited the efficiency of respiratory pectinirhombs in larger individuals and that rhombs increased in size to compensate. A likely explanation is that oxygen was depleted from the sea water as it moved through the pectinirhombs, shown schematically in Figure 2.29c. By the time a parcel of water, initially rich in oxygen, passed through the entire length of a rhomb, much of its oxygen would have been removed. Thus, the ability of the downstream end of the rhomb to extract oxygen would have been substantially less than that of the upstream end. This effect would have been less important in smaller individuals with smaller rhombs.

continued on next page

Box 2.3 (continued)

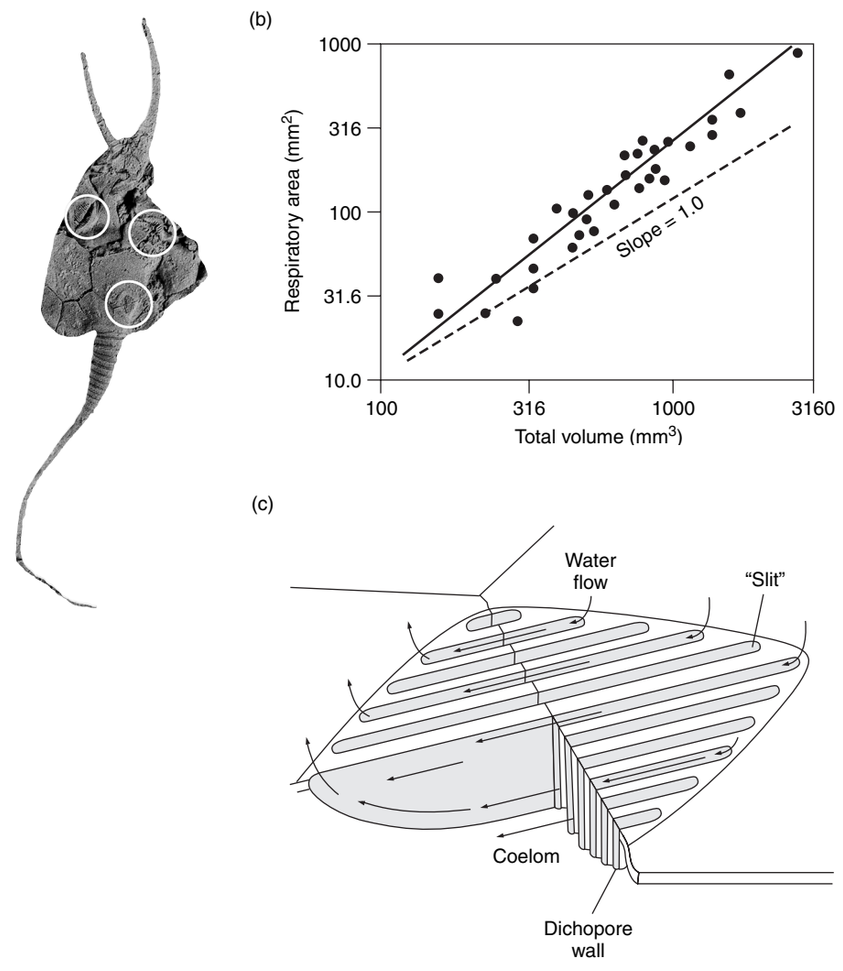

FIGURE 2.29 Allometric growth in an Ordovician rhombiferan echinoderm. (a) Individual with three pectinirhombs circled. (b) Scatterplot of total pectinirhomb area against thecal volume, both measured on a logarithmic scale. Each point is an individual of a different size. The dashed line of slope 1 is what we would expect to see for ideal allometric scaling in which rhomb area just keeps up with thecal volume as size increases. The solid line shows the actual relationship; it has a slope of 1.3, meaning that rhomb area is increasing at a faster size-specific rate than expected by a simple area:volume scaling. As explained in the text, this suggests that some factor limited pectinirhomb efficiency at larger sizes. (c) Schematic illustration of inferred pectinirhomb function. Pectinirhomb is shared between two thecal plates and contains a series of slits through which sea water flows. A thin wall at the base of the rhomb allows diffusion of dissolved gases between the sea water and the coelom (body cavity). *(From Brower, 1999)*

One of the best-known examples of an allometric relationship is that between brain mass and body mass in vertebrates. Figure 2.30 depicts this relationship schematically through human growth. There are two conspicuous features here. First, around the time of birth, the slope of the allometric curve decreases, which reflects a major decrease in the rate of cell division of neurons. Second, the slope after birth is substantially less than 1; with little or no neuronal cell division, growth of the brain is greatly outpaced by growth of the body. The relationship shows negative allometry: Brain mass increases more slowly than does body mass, and the ratio of brain mass to body mass therefore decreases steadily through ontogeny. (Of course, this will come as no surprise to anybody who has noted the proportionally large size of a human baby's head compared with that of an adult.)

We also see a negative allometry of brain mass relative to body mass if we study **interspecific allometry**—the changing relationship between two body parts considered across many species. Figure 2.31 depicts brain and body mass for a number of living vertebrate species, as well as lines showing the relationship between brain and body mass within several kinds of vertebrates. These lines have a slope of about 0.67. Although the reason for this is unclear, the fact that the slope is a simple ratio (2:3) suggests that it may be determined in part by an area-to-volume or other basic scaling relationship. The groups of points are also offset from one another. In terms of the allometric equation, they have the same value of the slope a, namely 0.67, but they have different values of b. What this means is that mammals and birds generally have larger brains for a given body size than do other vertebrates.

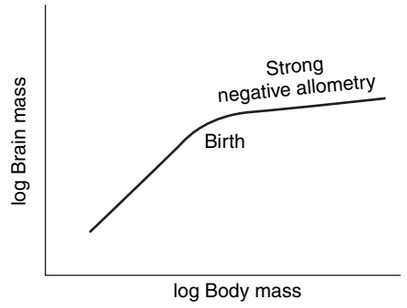

FIGURE 2.30 Idealized relationship between log brain mass and log body mass during human ontogeny. Initially, both masses increase at comparable size-specific rates, but the relative growth rate of brain mass is greatly reduced around the time of birth. *(After Lande, 1979)*

Species that fall above or below the line of allometry for their group have larger or smaller brains relative to what would be expected from their body mass alone; such species are referred to as more or less *encephalized*. Primates, for example, are highly encephalized among mammals, and humans are highly encephalized among primates.

Considering interspecific allometry can help us interpret differences in form between species when these differences are highly correlated with size. For example, large dinosaurs have a relatively small ratio of brain mass to body mass. This fact by itself, however, does not imply that dinosaurs were especially poorly encephalized. To determine the degree of encephalization, it is necessary to compare dinosaurs with the general trend for reptiles (Figure 2.32).

In living reptiles, brain mass and body mass can be measured directly; somewhat less direct means must be used for the extinct dinosaurs. Body mass can be estimated from skeletal measures because body mass and bone dimensions are correlated [SEE SECTION 3.2]. Similarly, brain mass can be estimated from cranial volume.

When dinosaurs are plotted along with other reptiles, it is clear that they represent a continuation of the allometric trend. The low ratio of brain mass to body mass for large dinosaurs is not a sign of unusually low encephalization but is instead exactly what one would expect for large reptiles in light of the negative allometry of brain size relative to body size.

Heterochrony

The study of anisometric growth has been closely tied to the concept of **heterochrony,** or evolutionary changes in the timing of development. Important aspects of developmental timing include growth rate and the onset of sexual maturity relative to growth of the body.

The principal reason heterochrony is biologically significant is that it may be a way to achieve a large

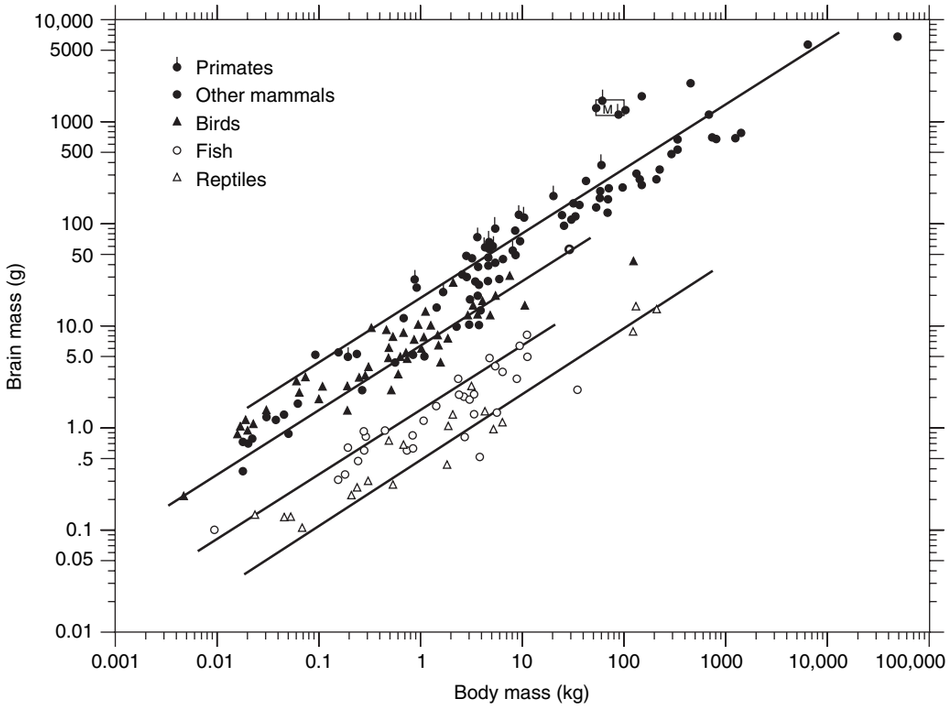

FIGURE 2.31 Comparison between brain mass and body mass for some groups of vertebrates. Both axes are logarithmic. Each species is represented by a single point, except for modern humans, which are represented by the range of variation indicated by the rectangle marked M. Within each group, the data show a trend with a slope approximating 2:3. *(From Jerison, 1969)*

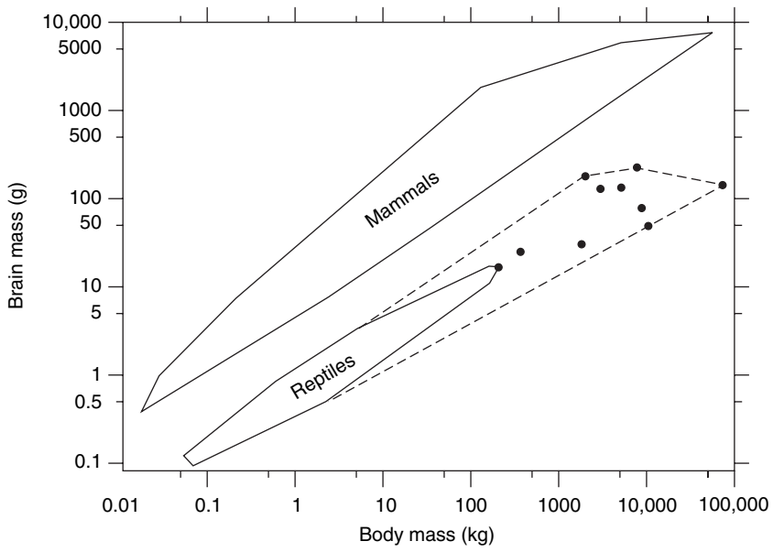

FIGURE 2.32 Comparison between brain mass and body mass for living reptiles and for dinosaurs, with mammals included for comparison. Both axes are logarithmic. The solid polygons enclose the range of variation for living species within mammals and living reptiles, as shown in Figure 2.31. The solid points are dinosaur species. The dashed polygon enclosing them can be interpreted as an extension of the field for living reptiles. *(From Jerison, 1969)*

evolutionary change in organismal morphology with a relatively small change in the underlying developmental pathway from juvenile to adult. If many traits are under common genetic control, natural selection [SEE SECTION 3.1] for size, growth rate, or some other underlying factor that affects many traits may bring with it numerous correlated changes in form.

Despite the attention paid to heterochrony as a potential mechanism for evolutionary change, it has been difficult to demonstrate it rigorously and to deduce the specific mechanisms that cause it. There are two main reasons for this. First, to be certain that a difference between two species reflects evolutionary change from one to the other, it is necessary to document ancestral–descendant relationships reliably (see Chapter 4). Second, a complete understanding of the mechanism of heterochrony often requires that we measure absolute growth rates with respect to age. This stands in contrast to our initial consideration of allometry, in which we compared the growth of two features to each other rather than to absolute age.

To see why this is so, consider the Lower Jurassic bivalve **lineage** *Gryphaea*, which shows the style of heterochrony known as **paedomorphosis.** In paedomorphosis, development evolves so that descendant adults resemble ancestral juveniles. (**Peramorphosis,** by constrast, is a kind of heterochrony in which the development of the descendant proceeds further than that of the ancestor, with the result that juvenile stages of the descendant resemble

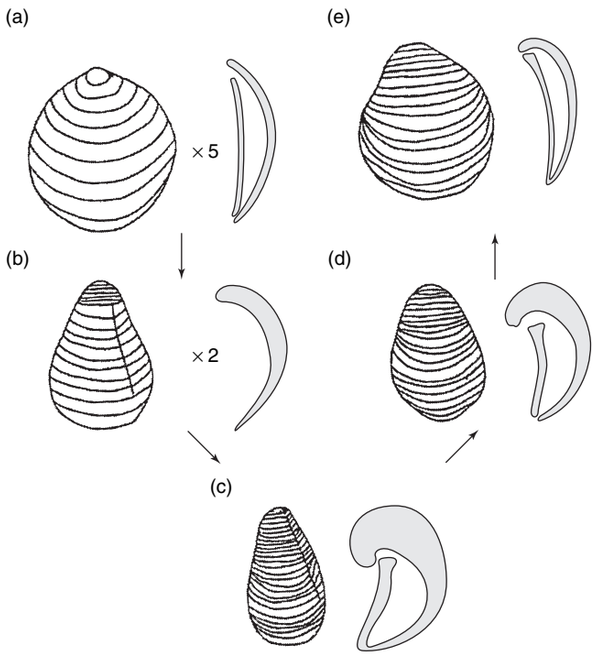

FIGURE 2.33 Heterochrony in a lineage of Lower Jurassic *Gryphaea*. The sequence labeled (a) through (c) shows ontogenetic development of the species *G. arcuata* from early juvenile through adult. The sequence labeled (c) through (e) shows evolutionary change in adult form, from (c) *G. arcuata* to (d) *G. mccullochi* to (e) *G. gigantea*. Each figure shows the exterior of the larger, left valve and a cross section through both valves. Note that the adults of *G. gigantea* resemble juveniles of *G. arcuata*. *(From Jones & Gould, 1999)*

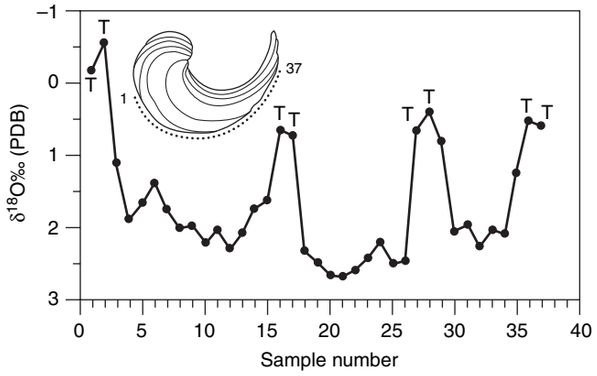

FIGURE 2.34 Variation in the oxygen isotopic composition of shell carbonate throughout the growth of an individual of *Gryphaea arcuata*. The inset shows a sketch of a shell, in which the direction of growth was to the right. The dots along the lower edge of this shell show 37 points at which shell samples were taken for chemical analysis. The plot compares measured oxygen isotopes of shell carbonate to the sample number. The notation "δ^{18}O‰(PDB)" expresses the ratio of ^{18}O to ^{16}O with reference to a standard of known composition [SEE SECTION 9.5]. Higher values (toward the bottom of the graph) indicate a larger ratio of ^{18}O to ^{16}O, which implies shell secretion at cooler temperatures. The sample points marked T are translucent shell increments that correspond to slow growth in the summer months. Three temperature cycles, indicating three annual cycles of shell growth, are shown here. *(From Jones & Gould, 1999)*

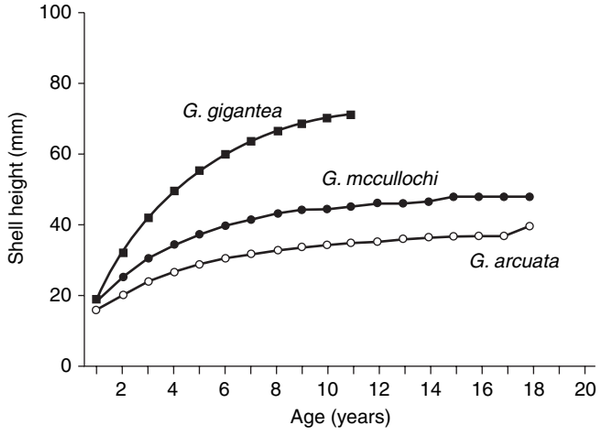

FIGURE 2.35 Average growth curves showing shell height against time for three species of *Gryphaea*. This shows that *G. gigantea* individuals grew for a shorter period of time, but at a higher rate, than those of *G. arcuata*. *(From Jones & Gould, 1999)*

ancestral adults.) In the *Gryphaea* lineage, the transition from *Gryphaea arcuata* to *G. mccullochi* to *G. gigantea* (Figure 2.33) involves striking changes in shape. The adults of the descendant *G. gigantea* resemble juveniles of the ancestral *G. arcuata* in being broad and flat in profile and less tightly coiled (Figure 2.33). These evolutionary changes appear to have a functional basis. Experimental flow-tank studies have verified that larger shells, with the shape of *G. arcuata* juveniles, are more stable on soft substrates such as those on which *Gryphaea* lived.

That the *Gryphaea* lineage underwent paedomorphic heterochrony seems clear, but, developmentally, how was the juvenile-like morphology produced in the ontogeny of *G. gigantea?* Did individuals develop over the same or a longer growth period than individuals of the ancestral species, but at a slower rate of shape change? Alternatively, did *G. gigantea* individuals grow more rapidly for a shorter interval of time? Clearly, either possibility could yield a paedomorphic adult, one with a large size but still retaining the juvenile form.

To distinguish these very different possibilities, it is necessary to analyze absolute age and growth rates. Fortunately, the age of individuals can be determined by chemical analysis of shells. It is well known from observations on a wide range of living aquatic organisms that the two most abundant **isotopes** of oxygen, ^{16}O and ^{18}O, are incorporated into the carbonate of shells in relative proportions that depend in part on ambient water temperature, with heavier isotopes preferentially incorporated at lower temperatures [SEE SECTION 9.5]. This effect is dictated by basic thermodynamics. Because of seasonal variation in water temperature, there is a regular variation in the ratio of ^{18}O to ^{16}O incorporated into the shell, as illustrated in Figure 2.34 for a specimen of one of the *Gryphaea* species. It is therefore possible to determine the number of seasonal cycles through which a shell has passed, and thus its age. Doing this for the three species of *Gryphaea* shows that *G. gigantea* grew for fewer years than did its ancestors, but at a substantially higher rate of size increase, before attaining its adult form (Figure 2.35). Thus, the precise nature of the evolutionary change via heterochrony was identified in this instance: The descendant form grew more rapidly for a shorter period of time.

2.4 CONCLUDING REMARKS

Although paleontologists have a wide range of tools readily available for describing and measuring form and ontogeny, these methods are still being developed at a rapid

pace. It will be interesting to see in the coming years which approaches prove most useful and for which questions.

Continued improvements in the measurement of absolute growth rates will enable the evolution of development to be studied more precisely, as in the *Gryphaea* example. Note that in this example we have accepted the ancestral–descendant relationships as given in Figure 2.33 and have bypassed the important question of how these relationships are known. In fact, how to determine the genealogy of evolving lineages is one of the most important issues in biology and paleontology. This subject will be taken up in Chapter 4.

The *Gryphaea* study is a success insofar as it clarifies the nature of evolutionary change by reconstructing growth relative to absolute age. Like most studies of heterochrony, however, it is limited to just a few traits. We would like to know whether heterochrony has molded a broad range of features in evolving lineages. Studies that consider a large suite of traits are only now becoming common. In some cases, it has been found that many traits simultaneously evolve by heterochrony; thus, the idea of achieving a large evolutionary change from a small developmental change is tenable. In other cases, however, the evolution of form is far more complex, with different parts of the organism evolving in different ways, some heterochronic, some not. For example, structures may shift in position in ways that cannot easily be explained by simple changes in the timing of development. In light of these studies, an important question for the future is just how important heterochrony really is in the evolution of form.

SUPPLEMENTARY READING

Feldmann, R. M., Chapman, R. E., and Hannibal, J. T. (1989) *Paleotechniques* (Paleontological Society Special Publication Number 4). Knoxville, Tenn., The University of Tennessee, 358 pp. [A series of papers on preparation and illustration of fossil specimens.]

Gould, S. J. (1977) *Ontogeny and Phylogeny*. Cambridge, Mass., Harvard University Press, 501 pp. [Authoritative historical review of the study of allometry, heterochrony, and related topics.]

Kummel, B. H., and Raup, D. M. (eds.) (1965) *Handbook of Paleontological Techniques*. San Francisco, W. H. Freeman and Company, 852 pp. [A collection of specialized articles on a range of techniques for collecting, preparing, and illustrating paleontological material.]

McKinney, M. L. (ed.) (1988) *Heterochrony in Evolution: A Multidisciplinary Approach*. New York, Plenum, 348 pp. [A series of papers on general methods for studying development and evolution, with applications to a range of organisms.]

Rohlf, F. J., and Bookstein, F. L. (eds.) (1990) *Proceedings of the Michigan Morphometrics Workshop*. (University of Michigan Museum of Zoology Special Publication Number 2.) Ann Arbor, Mich., University of Michigan, 380 pp. [Pragmatic overview of methods for measuring and analyzing form.]

Schmidt-Nielsen, K. (1984) *Scaling: Why is Animal Size So Important?* Cambridge, U.K., Cambridge University Press, 241 pp. [Important overview of the effects of body size on function and physiology of animals.]

Thompson, D'A. W. (1942) *On Growth and Form*. Cambridge, U.K., Cambridge University Press, 1116 pp. [Classic work on ontogeny and other aspects of organic form. Essential reading for all interested in the interpretation of form.]

Wolpert, L., Beddington, R., Jessell, T., Lawrence, P., Meyerowitz, E., and Smith, J. (2001) *Principles of Development,* 2nd ed. Oxford, U.K., Oxford University Press, 568 pp. [Comprehensive text on developmental biology.]

Zelditch, M. L. (ed.) (2001) *Beyond Heterochrony: The Evolution of Development*. New York, Wiley-Liss, 371 pp. [A series of case studies of developmental change in evolution.]

SOFTWARE

National Institutes of Health. NIH Image, http://rsb.info.nih.gov/nih-image/ [Software for digitizing and analyzing images.]

Rohlf, F. J. tpsDIG, http://life.bio.sunysb.edu/morph/ [Software for digitizing images and analyzing outlines and landmarks.]